Atmospheric Physics seminar

The effect of lubrication forces on the collision statistics of cloud droplets in homogeneous isotropic turbulence

Institute of Meteorology and Water Management, National Research Institute (IMGW–PIB, Warsaw)

Institute of Geophysics, University of Warsaw (IGF UW, Warsaw)

April 30th, 2021

Overview

Collision-coalescence of inertial particles in turbulent flows

- Turbulent flows and particle transport are very common phenomena in nature. The processes occur continuously, with different intensity and at different scales.
- Particle transport by a turbulent fluid phase is also an important mechanism for many technological processes (combustion of pulverized coal in boilers, pneumatic transport in pipelines, combustion of the fuel in engines or spraying of fertilizers and plant protection products)
- In this study, the general focus is on modeling of cloud microphysical processes.

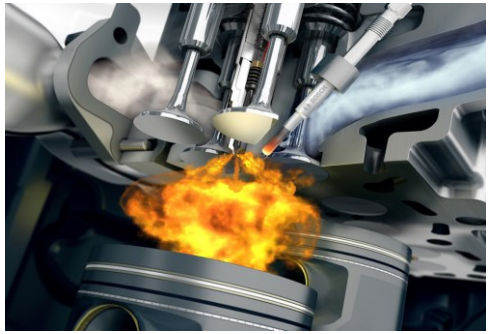

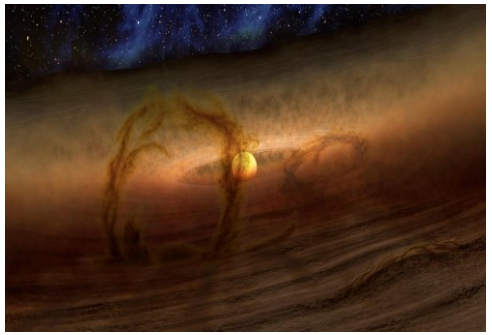

"Warm rain processes account for about **31%** of the total rain fall and **72%** of the total rain area in tropics. This process is active in most climate zones in all seasons."

Motivation of study:

To compute kinematics and collision statistics of water droplets typical of atmospheric clouds

Focus of study:

To investigate the effect of lubrication forces on the dynamics of aerodynamically interacting droplets

Problem definition

Motion of particles in homogeneous isotropic turbulence

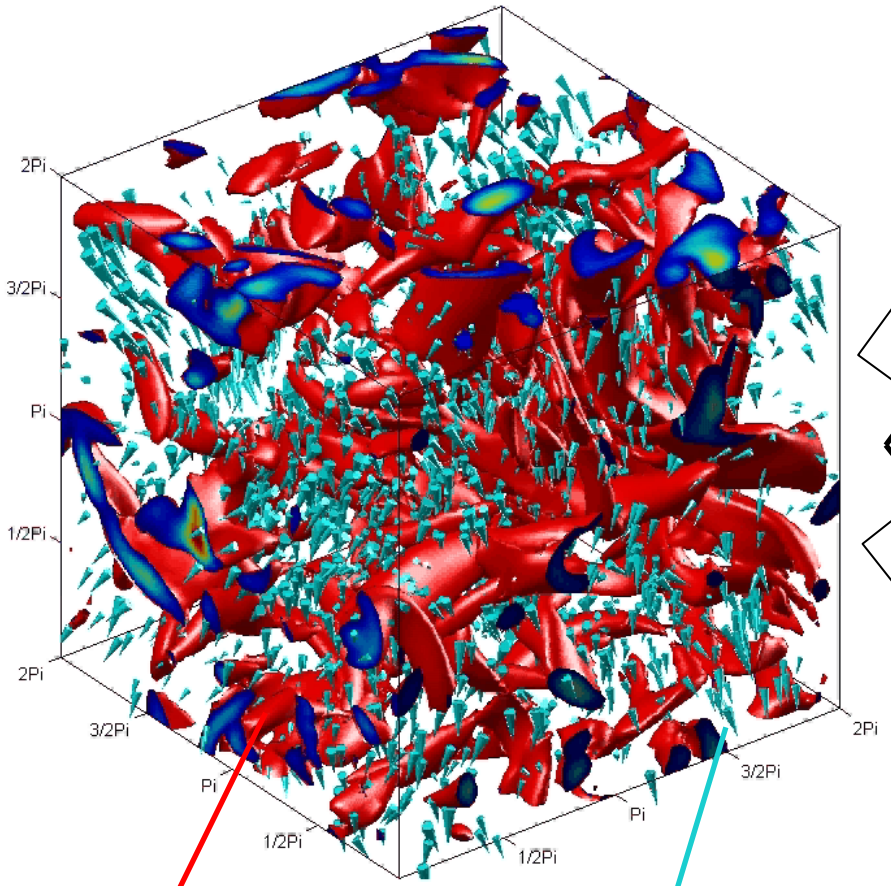

Contours of vorticity
(Color: magnitude)

Motion of particles
(Cone: velocity magnitude and direction)

Continuous phase

Dispersed phase

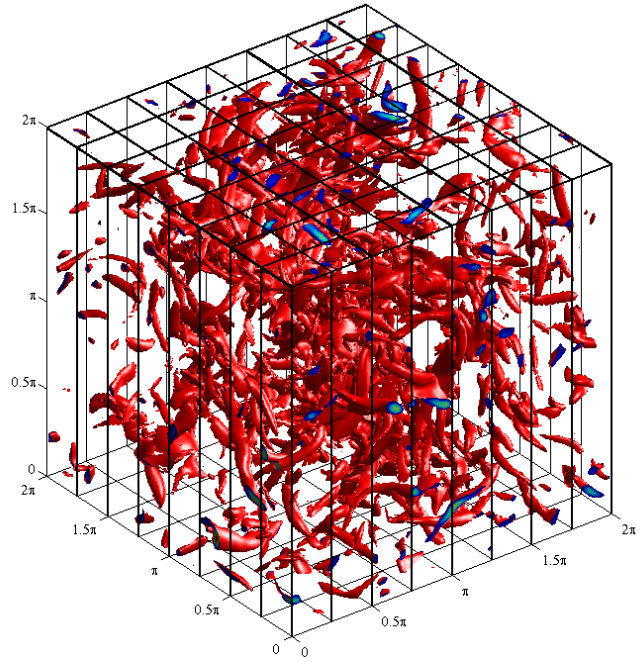

Turbulent background flow $\boldsymbol{U}(\boldsymbol{x}, t)$

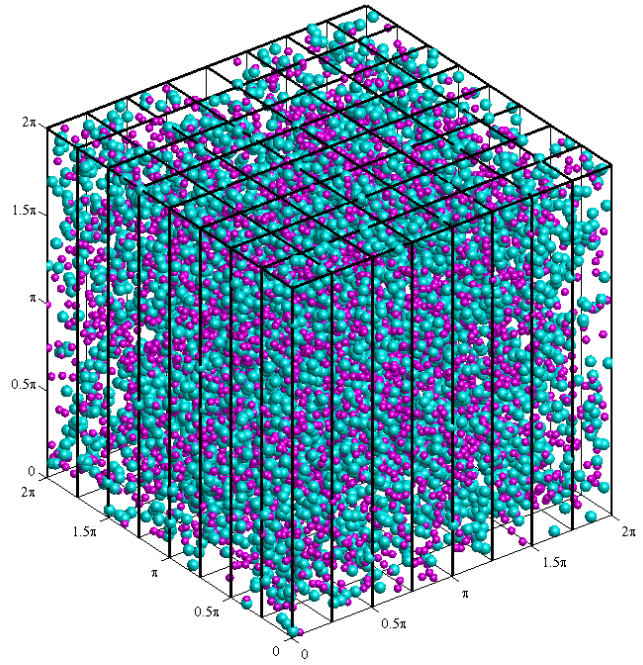

Particle motion $\boldsymbol{Y}^{(k)}(t)$, $\boldsymbol{V}^{(k)}(t)$

Problem definition

Simulation of the homogeneous isotropic turbulence (HIT)

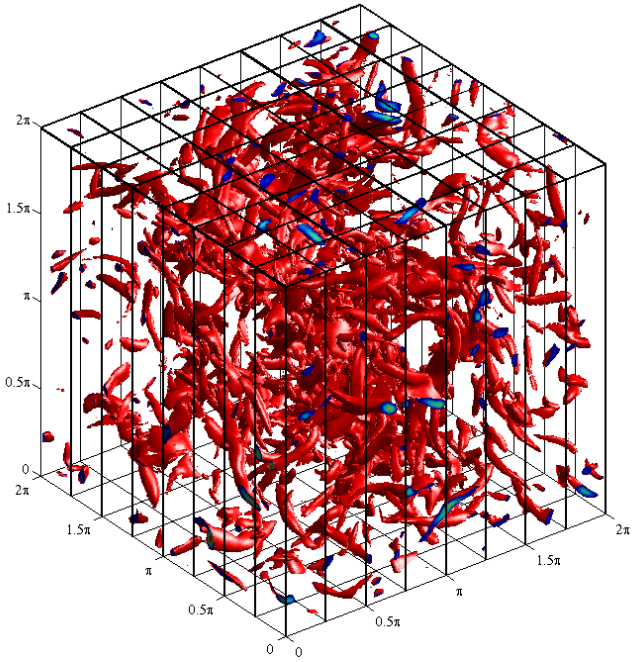

- Governing equations

$$\frac{\partial \boldsymbol{U}}{\partial t} = \boldsymbol{U}\times\boldsymbol{\omega} - \nabla\left(\frac{P}{\rho} + \frac{1}{2}\boldsymbol{U}^2\right) + \nu\nabla^2\boldsymbol{U} + \boldsymbol{f}(\boldsymbol{x},t)$$

$$\nabla\cdot\boldsymbol{U} = 0$$

where vorticity $\boldsymbol{\omega} = \nabla\times\boldsymbol{U}$

$$= \left(\frac{\partial w}{\partial y} - \frac{\partial v}{\partial z}\right)\vec{i} + \left(\frac{\partial u}{\partial z} - \frac{\partial w}{\partial x}\right)\vec{j} + \left(\frac{\partial v}{\partial x} - \frac{\partial u}{\partial y}\right)\vec{k}$$

- Basic assumptions

3D incompressible homogeneous isotropic turbulent flow with periodic boundary conditions (also for droplets) on a cube of size 2π

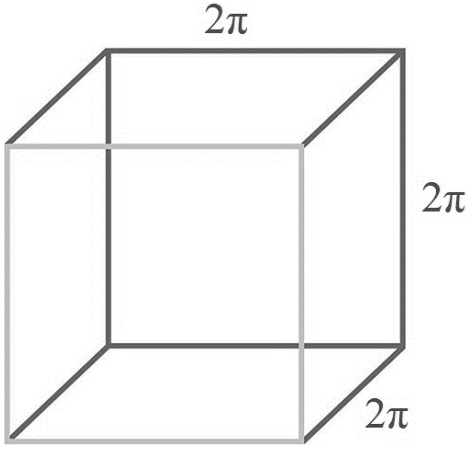

- Discretization (Eulerian)

3D Cartesian mesh of *N* equally spaced grid points in each spatial direction

- Solution Method

Pseudo-spectral method for direct numerical simulation (DNS)
The momentum equation is solved (integrated) in the spectral space using discrete Fourier transform as

$$\boldsymbol{U}(\boldsymbol{x},t) = \sum_{k_1}\sum_{k_2}\sum_{k_3}\hat{\boldsymbol{U}}(\boldsymbol{k},t)e^{i(k_1x+k_2y+k_3z)} \equiv \sum_{\boldsymbol{k}}\hat{\boldsymbol{U}}(\boldsymbol{k},t)e^{i\boldsymbol{k}\cdot\boldsymbol{x}}$$

where $k_i = 0,\pm1,\pm2,...,\pm\frac{N}{2}$

and $\hat{\boldsymbol{\omega}}(\boldsymbol{k},t) = i\,\boldsymbol{k}\times\hat{\boldsymbol{U}}(\boldsymbol{k},t)$. The inverse Fourier transform is

$$\hat{\boldsymbol{U}}(\boldsymbol{k},t) = \frac{1}{N^3}\sum_{\boldsymbol{x}}\boldsymbol{U}(\boldsymbol{x},t)e^{-i\boldsymbol{k}\cdot\boldsymbol{x}}$$

$$= \frac{1}{N^3}\sum_{j=0}^{N-1}\sum_{m=0}^{N-1}\sum_{n=0}^{N-1}\boldsymbol{U}\left(x_j = \frac{2\pi j}{N}, y_m = \frac{2\pi m}{N}, z_n = \frac{2\pi n}{N}, t\right)$$

$$\times e^{-i\left(2\pi jk_1/N + 2\pi mk_2/N + 2\pi nk_3/N\right)}$$

Problem definition

Algorithm for simulating the HIT

Solution

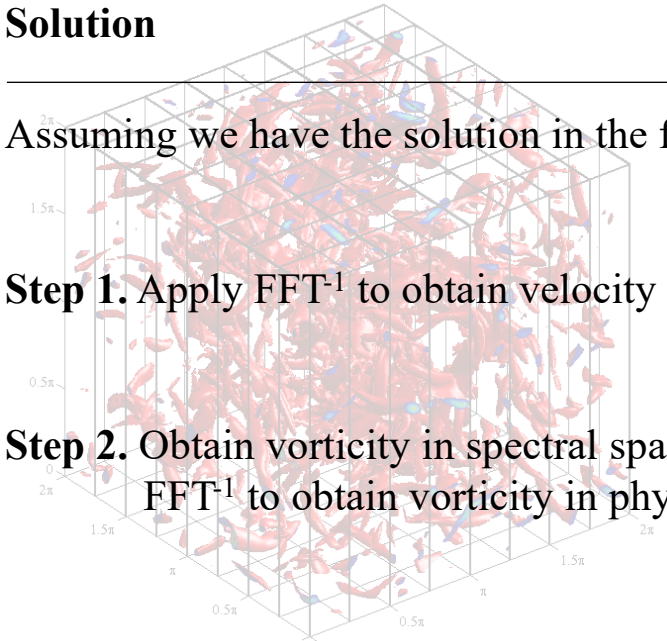

Assuming we have the solution in the following form

Step 1. Apply FFT^{-1} to obtain velocity in physical space

Step 2. Obtain vorticity in spectral space and then apply FFT^{-1} to obtain vorticity in physical space

Step 3. Calculate $\boldsymbol{N_1}(\boldsymbol{x}, t) \equiv \boldsymbol{U} \times \boldsymbol{\omega}$ (the first nonlinear term RHS of N–S) in physical space and FFT to spectral space

Step 4. Evolve the velocity in time

Note: $\boldsymbol{N_2}(\boldsymbol{x}, t) \equiv \nabla(P/\rho + U^2/2)$

in which $\hat{\boldsymbol{N}}_2(\boldsymbol{k},t) = -\dfrac{i\boldsymbol{k}\cdot\hat{\boldsymbol{N}}_1(\boldsymbol{k},t)}{k^2}$; Because $\nabla\cdot\boldsymbol{U}=0$

Algorithm

$$\hat{\boldsymbol{U}}(\boldsymbol{k},dt);\ \hat{\boldsymbol{U}}(\boldsymbol{k},2dt);\ \ldots;\ \hat{\boldsymbol{U}}(\boldsymbol{k},\mathrm{n}dt) \xrightarrow{\text{To compute}} \hat{\boldsymbol{U}}(\boldsymbol{k},(\mathrm{n}+1)dt)$$

$$\hat{\boldsymbol{U}}(\boldsymbol{k},t) \xrightarrow{\text{FFT}^{-1}} \boldsymbol{U}(\boldsymbol{x},t)$$

$$\hat{\boldsymbol{\omega}}(\boldsymbol{k},t) = i\boldsymbol{k}\times\hat{\boldsymbol{U}}(\boldsymbol{k},t) \xrightarrow{\text{FFT}^{-1}} \boldsymbol{\omega}(\boldsymbol{x},t)$$

$$\boldsymbol{U}(\boldsymbol{x},\mathrm{n}dt)\times\boldsymbol{\omega}(\boldsymbol{x},\mathrm{n}dt) \xrightarrow{\text{FFT}} \hat{\boldsymbol{N}}_1(\boldsymbol{k},\mathrm{n}dt)$$

Adams–Bashforth (AB2)

$$\hat{\boldsymbol{U}}(\boldsymbol{k},(\mathrm{n}+1)dt) - \hat{\boldsymbol{U}}(\boldsymbol{k},\mathrm{n}dt) = \frac{3}{2}\hat{\boldsymbol{N}}_1(\boldsymbol{k},\mathrm{n}dt)dt - \frac{1}{2}\hat{\boldsymbol{N}}_1(\boldsymbol{k},(\mathrm{n}\text{-}1)dt)dt$$

$$-i\boldsymbol{k}\cdot\hat{\boldsymbol{N}}_2(\boldsymbol{k},(\mathrm{n}+1)dt)dt$$

Crank–Nicolson $\longleftarrow$ $-\dfrac{1}{2}\nu k^2\left(\hat{\boldsymbol{U}}(\boldsymbol{k},\mathrm{n}dt) + \hat{\boldsymbol{U}}(\boldsymbol{k},(\mathrm{n}+1)dt)\right)dt$

Euler $\longleftarrow$ $+\hat{\boldsymbol{f}}(\boldsymbol{k},\mathrm{n}dt)dt$ $\longrightarrow$ Deterministic

Problem definition

Evolution of the dispersed phase and aerodynamic interactions

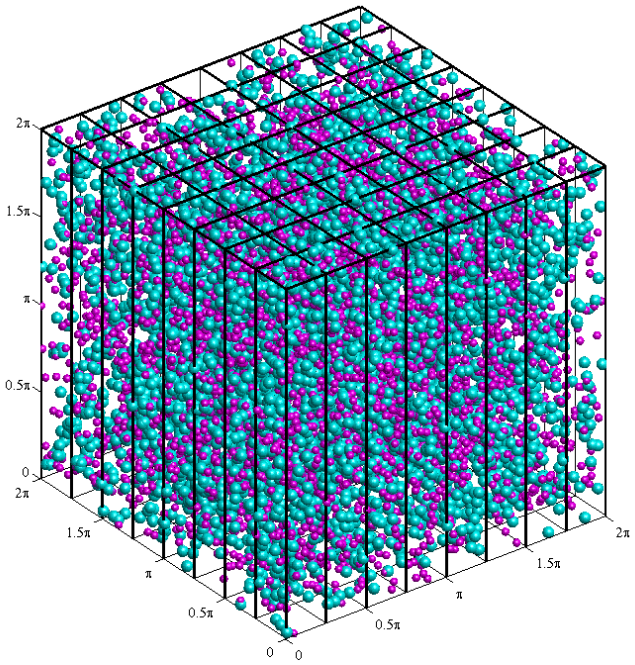

- Governing equations (typical):

$$\frac{\mathrm{d}\boldsymbol{V}^{(k)}(t)}{\mathrm{d}t} = -\frac{\boldsymbol{V}^{(k)}(t) - \boldsymbol{U}(\boldsymbol{Y}^{(k)}(t),\, t)}{\tau_p^{(k)}} + \boldsymbol{g}$$

$$\frac{\mathrm{d}\boldsymbol{Y}^{(k)}(t)}{\mathrm{d}t} = \boldsymbol{V}^{(k)}(t)$$

For k-th particle: $\boldsymbol{V}^{(k)}(t)$ is the particle velocity, $\tau_p{}^{(k)}$ is its Stokes inertial response time, and $\boldsymbol{U}(\boldsymbol{Y}^{(k)}(t), t)$ is the undisturbed fluid velocity, $\boldsymbol{U}(\boldsymbol{x}, t)$, at the location of the particle: $\boldsymbol{Y}^{(k)}(t)$

+ AIs →

Limitation: using this set of equations, the effect of interaction among particles would be overlooked

- Aerodynamic interactions (AIs):

Two droplets sedimenting under gravity in still air

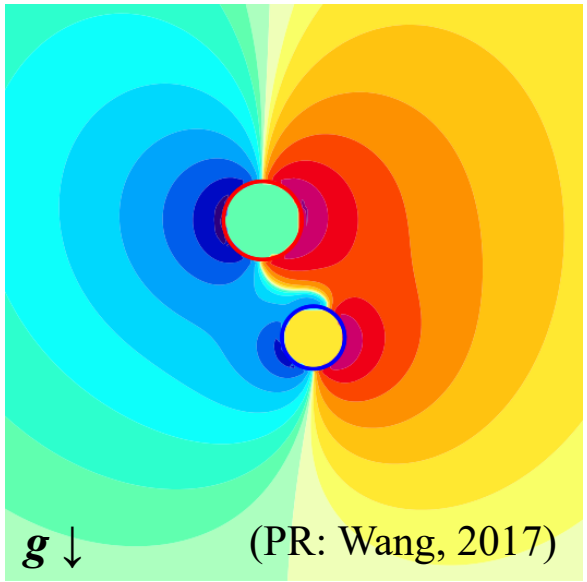

The motion of each droplet is generating a perturbation field that induces a disturbance velocity at the location of the other droplet

- Equations of motion considering AIs:

$$\frac{\mathrm{d}\boldsymbol{V}^{(k)}(t)}{\mathrm{d}t} = -\frac{\boldsymbol{V}^{(k)}(t) - \left(\boldsymbol{U}^{(k)} + \underline{\boldsymbol{u}}^{(k)}\right)}{\tau_p^{(k)}} + \boldsymbol{g}$$

$$\frac{\mathrm{d}\boldsymbol{Y}^{(k)}(t)}{\mathrm{d}t} = \boldsymbol{V}^{(k)}(t)$$

where $\boldsymbol{u}^{(k)}$ is the disturbance velocity felt at the location of k-th particle, and $\boldsymbol{U}^{(k)} = \boldsymbol{U}(\boldsymbol{Y}^{(k)}(t), t)$.

Aerodynamic interactions

How to determine?

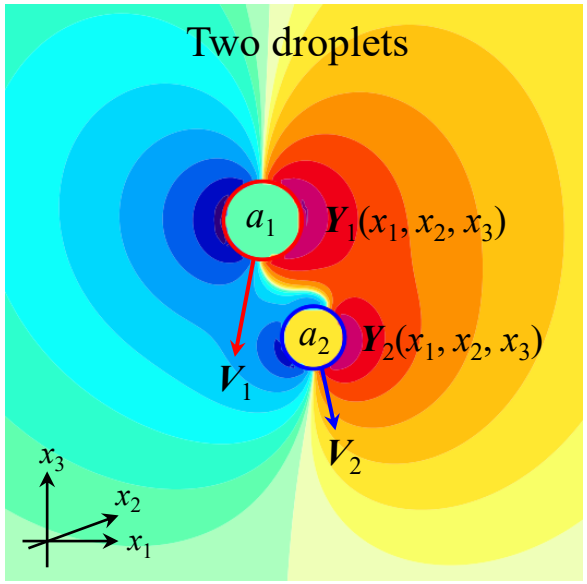

2 droplets

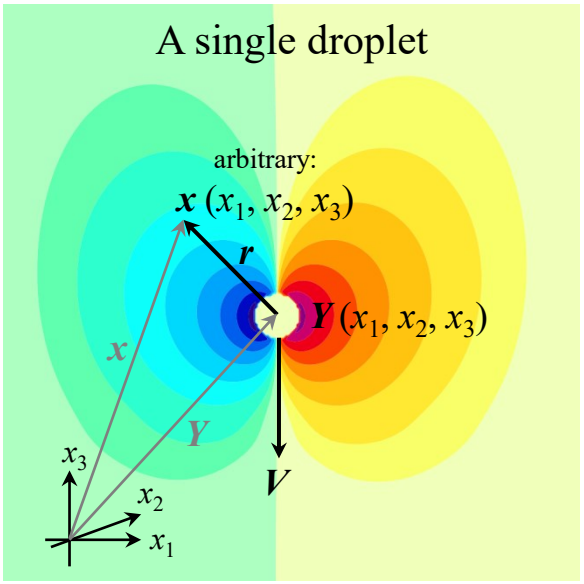

n droplets

N-body ISM?

Mathematical description of disturbance fields induced by particles using the solution to Stokes equation

Perturbation field for:	Mathematical description	Position vectors*
A single droplet	$\boldsymbol{u}(\boldsymbol{x},t)=\boldsymbol{u}_{\mathrm{St}}(\boldsymbol{r};a,\boldsymbol{V})=\left(\frac{3}{4}\frac{a}{r}-\frac{3}{4}\left(\frac{a}{r}\right)^3\right)\frac{\boldsymbol{r}}{r^2}(\boldsymbol{r}\cdot\boldsymbol{V})+\left(\frac{3}{4}\frac{a}{r}+\frac{1}{4}\left(\frac{a}{r}\right)^3\right)\boldsymbol{V}=\Lambda\boldsymbol{r}(\boldsymbol{r}\cdot\boldsymbol{V})+\beta\boldsymbol{V}$	$\boldsymbol{r}=\boldsymbol{x}-\boldsymbol{Y}$
Two droplets using (original) superposition method	$\boldsymbol{u}(\boldsymbol{x},t)=\boldsymbol{u}_{\mathrm{St}}\left(\boldsymbol{r}_1;a_1,\boldsymbol{V}_1-\boldsymbol{u}_{\mathrm{St}}(\boldsymbol{Y}_1-\boldsymbol{Y}_2;a_2,\boldsymbol{V}_2)\right)+\boldsymbol{u}_{\mathrm{St}}\left(\boldsymbol{r}_2;a_2,\boldsymbol{V}_2-\boldsymbol{u}_{\mathrm{St}}(\boldsymbol{Y}_2-\boldsymbol{Y}_1;a_1,\boldsymbol{V}_1)\right)$	
Two droplets using improved superposition method (ISM)	$\boldsymbol{u}(\boldsymbol{x},t)=\boldsymbol{u}_{\mathrm{St}}\left(\boldsymbol{r}_1;a_1,\boldsymbol{V}_1-\underbrace{\boldsymbol{u}_{\mathrm{St}}(\boldsymbol{Y}_1-\boldsymbol{Y}_2;a_2,\boldsymbol{V}_2-\boldsymbol{u}_2)}_{\boldsymbol{u}_1}\right)+\boldsymbol{u}_{\mathrm{St}}\left(\boldsymbol{r}_2;a_2,\boldsymbol{V}_2-\underbrace{\boldsymbol{u}_{\mathrm{St}}(\boldsymbol{Y}_2-\boldsymbol{Y}_1;a_1,\boldsymbol{V}_1-\boldsymbol{u}_1)}_{\boldsymbol{u}_2}\right)$ $=\boldsymbol{u}_{\mathrm{St}}(\boldsymbol{r}_1;a_1,\boldsymbol{V}_1-\boldsymbol{u}_1)+\boldsymbol{u}_{\mathrm{St}}(\boldsymbol{r}_2;a_2,\boldsymbol{V}_2-\boldsymbol{u}_2)$	$\boldsymbol{r}_1=\boldsymbol{x}-\boldsymbol{Y}_1$ $\boldsymbol{r}_2=\boldsymbol{x}-\boldsymbol{Y}_2$

* The position relative to the center of the particle/droplet

Aerodynamic interactions

Extension of ISM to an arbitrary number of droplets (N_p) and hybrid DNS (HDNS)

Using ISM to compute disturbance velocities

Number of droplets	Disturbance velocity (perturbation felt at the location of droplet)	Flow
2	$\boldsymbol{u}_1 = \boldsymbol{u}_{St}\left(\boldsymbol{Y}_1 - \boldsymbol{Y}_2; a_2, \boldsymbol{V}_2 - \boldsymbol{u}_2\right)$ $\boldsymbol{u}_2 = \boldsymbol{u}_{St}\left(\boldsymbol{Y}_2 - \boldsymbol{Y}_1; a_1, \boldsymbol{V}_1 - \boldsymbol{u}_1\right)$	Still air
N_p	$\boldsymbol{u}^{(k)} = \sum_{\substack{m=1 \\ m\neq k}}^{N_p} \boldsymbol{u}_{St}\left(\boldsymbol{r}^{(k,m)^*}; a^{(m)}, \boldsymbol{V}^{(m)} - \boldsymbol{u}^{(m)}\right), \quad k^{**} = 1,2,\ldots,N_p$	Still air
N_p	$\boldsymbol{u}^{(k)} = \sum_{\substack{m=1 \\ m\neq k}}^{N_p} \boldsymbol{u}_{St}\left(\boldsymbol{r}^{(k,m)}; a^{(m)}, \boldsymbol{V}^{(m)} - \left(\underline{\boldsymbol{U}}^{(m)} + \underline{\boldsymbol{u}}^{(m)}\right)\right), \quad k = 1,2,\ldots,N_p$ ←	Turbulent flow field

* $\boldsymbol{r}^{(k,m)} = \boldsymbol{Y}^{(k)} - \boldsymbol{Y}^{(m)}$

** For an arbitrary droplet k, all the other droplets are indexed m

In the last equation let's move the unknowns, $\boldsymbol{u}^{(m)}$, to the LHS: $\boldsymbol{u}^{(k)} + \sum_{\substack{m=1 \\ m\neq k}}^{N_p} \boldsymbol{u}_{St}\left(\boldsymbol{r}^{(k,m)}; a^{(m)}, \boldsymbol{u}^{(m)}\right) = \sum_{\substack{m=1 \\ m\neq k}}^{N_p} \boldsymbol{u}_{St}\left(\boldsymbol{r}^{(k,m)}; a^{(m)}, \boldsymbol{V}^{(m)} - \boldsymbol{U}^{(m)}\right), \quad k = 1,2,\ldots,N_p.$

Now we define:

$$\Lambda^{(k,m)} \equiv \left(\frac{3}{4}\frac{a^{(m)}}{r^{(k,m)}} - \frac{3}{4}\left(\frac{a^{(m)}}{r^{(k,m)}}\right)^3\right) \Big/ r^{(k,m)^2}$$

$$\beta^{(k,m)} \equiv \left(\frac{3}{4}\frac{a^{(m)}}{r^{(k,m)}} + \frac{1}{4}\left(\frac{a^{(m)}}{r^{(k,m)}}\right)^3\right)$$

then:

$$\begin{aligned} \boldsymbol{u}_{St}^{(k,m)} &\equiv \boldsymbol{u}_{St}^{(k,m)}\left(\boldsymbol{r}^{(k,m)}; a^{(m)}, \boldsymbol{v}^{(m)}\right) \\ &= \Lambda^{(k,m)} \boldsymbol{r}^{(k,m)}\left(\boldsymbol{r}^{(k,m)} \cdot \boldsymbol{v}^{(m)}\right) + \beta^{(k,m)} \boldsymbol{v}^{(m)} \\ &= \alpha_{i,j}^{(k,m)} v_j^{(m)} \\ &\equiv \boldsymbol{\alpha}^{(k,m)} \boldsymbol{v}^{(m)} \end{aligned}$$

such that $\boldsymbol{\alpha}^{(k,m)}$ is a 3×3 symmetric matrix with components:

$$\alpha_{i,j}^{(k,m)} = \left(\Lambda r_i r_j + \beta \delta_{ij}\right)^{(k,m)} = \alpha_{j,i}^{(k,m)} \quad (m \neq k)$$

Aerodynamic interactions

HDNS

$$\frac{\mathrm{d}\boldsymbol{V}^{(k)}(t)}{\mathrm{d}t} = -\frac{\boldsymbol{V}^{(k)}(t) - \left(\boldsymbol{U}^{(k)} + \boldsymbol{u}^{(k)}\right)}{\tau_p^{(k)}} + \boldsymbol{g} \rightarrow \begin{cases} \boldsymbol{V}^{(k)} \rightarrow \text{Eqs. of motion} \\ \boldsymbol{U}^{(k)} \rightarrow \text{DNS} \\ \boldsymbol{u}^{(k)} \rightarrow N\text{-body ISM (?)} \end{cases} \rightarrow \text{HDNS}$$

Superposed Stokes disturbance velocities of $N_\mathrm{p} - 1$ droplets, $\boldsymbol{u}^{(k)}$, felt at the location of an arbitrary droplet k can be described as:

$$\boldsymbol{u}^{(k)} + \sum_{\substack{m=1 \\ m\neq k}}^{N_\mathrm{p}} \boldsymbol{u}_{\mathrm{St}}\left(\boldsymbol{r}^{(k,m)}; a^{(m)}, \boldsymbol{u}^{(m)}\right) = \sum_{\substack{m=1 \\ m\neq k}}^{N_\mathrm{p}} \boldsymbol{u}_{\mathrm{St}}\left(\boldsymbol{r}^{(k,m)}; a^{(m)}, \boldsymbol{V}^{(m)} - \boldsymbol{U}^{(m)}\right), \quad k = 1, 2, \ldots, N_\mathrm{p}.$$

It was shown: $\boldsymbol{u}_{\mathrm{St}}^{(k,m)} = \boldsymbol{\alpha}^{(k,m)} \boldsymbol{v}^{(m)}$

That is:

$$\begin{aligned}
\boldsymbol{I}_3\boldsymbol{u}^{(1)} + \boldsymbol{\alpha}^{(1,2)}\boldsymbol{u}^{(2)} + \cdots + \boldsymbol{\alpha}^{(1,N_\mathrm{p})}\boldsymbol{u}^{(N_\mathrm{p})} &= \boldsymbol{0}_3\left(\boldsymbol{V}^{(1)} - \boldsymbol{U}^{(1)}\right) + \boldsymbol{\alpha}^{(1,2)}\left(\boldsymbol{V}^{(2)} - \boldsymbol{U}^{(2)}\right) + \cdots + \boldsymbol{\alpha}^{(1,N_\mathrm{p})}\left(\boldsymbol{V}^{(N_\mathrm{p})} - \boldsymbol{U}^{(N_\mathrm{p})}\right) \\
\boldsymbol{\alpha}^{(2,1)}\boldsymbol{u}^{(1)} + \boldsymbol{I}_3\boldsymbol{u}^{(2)} + \cdots + \boldsymbol{\alpha}^{(2,N_\mathrm{p})}\boldsymbol{u}^{(N_\mathrm{p})} &= \boldsymbol{\alpha}^{(2,1)}\left(\boldsymbol{V}^{(1)} - \boldsymbol{U}^{(1)}\right) + \boldsymbol{0}_3\left(\boldsymbol{V}^{(2)} - \boldsymbol{U}^{(2)}\right) + \cdots + \boldsymbol{\alpha}^{(2,N_\mathrm{p})}\left(\boldsymbol{V}^{(N_\mathrm{p})} - \boldsymbol{U}^{(N_\mathrm{p})}\right) \\
&\vdots \\
\boldsymbol{\alpha}^{(N_\mathrm{p},1)}\boldsymbol{u}^{(1)} + \boldsymbol{\alpha}^{(N_\mathrm{p},2)}\boldsymbol{u}^{(2)} + \cdots + \boldsymbol{I}_3\boldsymbol{u}^{(N_\mathrm{p})} &= \boldsymbol{\alpha}^{(N_\mathrm{p},1)}\left(\boldsymbol{V}^{(1)} - \boldsymbol{U}^{(1)}\right) + \boldsymbol{\alpha}^{(N_\mathrm{p},2)}\left(\boldsymbol{V}^{(2)} - \boldsymbol{U}^{(2)}\right) + \cdots + \boldsymbol{0}_3\left(\boldsymbol{V}^{(N_\mathrm{p})} - \boldsymbol{U}^{(N_\mathrm{p})}\right)
\end{aligned}$$

where $\boldsymbol{I}_3 = \begin{bmatrix} 1 & 0 & 0 \\ 0 & 1 & 0 \\ 0 & 0 & 1 \end{bmatrix}$ and $\boldsymbol{0}_3 = \begin{bmatrix} 0 & 0 & 0 \\ 0 & 0 & 0 \\ 0 & 0 & 0 \end{bmatrix}$

and each row consists of 3 equations along 3 spatial directions. Thus, this set of $3N_\mathrm{p}$ equations in a compact notation can be described as:

$$\underbrace{\begin{bmatrix} \boldsymbol{I}_3 & \cdots & \boldsymbol{\alpha}^{(1,m)} & \cdots & \boldsymbol{\alpha}^{(1,N_\mathrm{p})} \\ \vdots & \ddots & \vdots & \ddots & \vdots \\ \boldsymbol{\alpha}^{(k,1)} & \cdots & \boldsymbol{\alpha}^{(k,m)} & \cdots & \boldsymbol{\alpha}^{(k,N_\mathrm{p})} \\ \vdots & \ddots & \vdots & \ddots & \vdots \\ \boldsymbol{\alpha}^{(N_\mathrm{p},1)} & \cdots & \boldsymbol{\alpha}^{(N_\mathrm{p},m)} & \cdots & \boldsymbol{I}_3 \end{bmatrix}}_{\boldsymbol{A}} \underbrace{\begin{pmatrix} \boldsymbol{u}^{(1)} \\ \vdots \\ \boldsymbol{u}^{(m)} \\ \vdots \\ \boldsymbol{u}^{(N_\mathrm{p})} \end{pmatrix}}_{\boldsymbol{x}} = \underbrace{\begin{bmatrix} \boldsymbol{0}_3 & \cdots & \boldsymbol{\alpha}^{(1,m)} & \cdots & \boldsymbol{\alpha}^{(1,N_\mathrm{p})} \\ \vdots & \ddots & \vdots & \ddots & \vdots \\ \boldsymbol{\alpha}^{(k,1)} & \cdots & \boldsymbol{\alpha}^{(k,m)} & \cdots & \boldsymbol{\alpha}^{(k,N_\mathrm{p})} \\ \vdots & \ddots & \vdots & \ddots & \vdots \\ \boldsymbol{\alpha}^{(N_\mathrm{p},1)} & \cdots & \boldsymbol{\alpha}^{(N_\mathrm{p},m)} & \cdots & \boldsymbol{0}_3 \end{bmatrix}}_{\boldsymbol{B}} \underbrace{\begin{pmatrix} \boldsymbol{V}^{(1)} - \boldsymbol{U}^{(1)} \\ \vdots \\ \boldsymbol{V}^{(m)} - \boldsymbol{U}^{(m)} \\ \vdots \\ \boldsymbol{V}^{(N_\mathrm{p})} - \boldsymbol{U}^{(N_\mathrm{p})} \end{pmatrix}}_{\boldsymbol{y}}$$

$(k \neq m)$, so $\boldsymbol{A} = \boldsymbol{B} + \boldsymbol{I}_{N_\mathrm{p}}$

Parallel GMRes solver

Aerodynamic interactions

Inaccurate force representation of ISM

Focus of our study

Lubrication effect:

$s - 2 \rightarrow 0$ then $F \rightarrow \infty$ (singular)

so strong dependency to Δt is expected

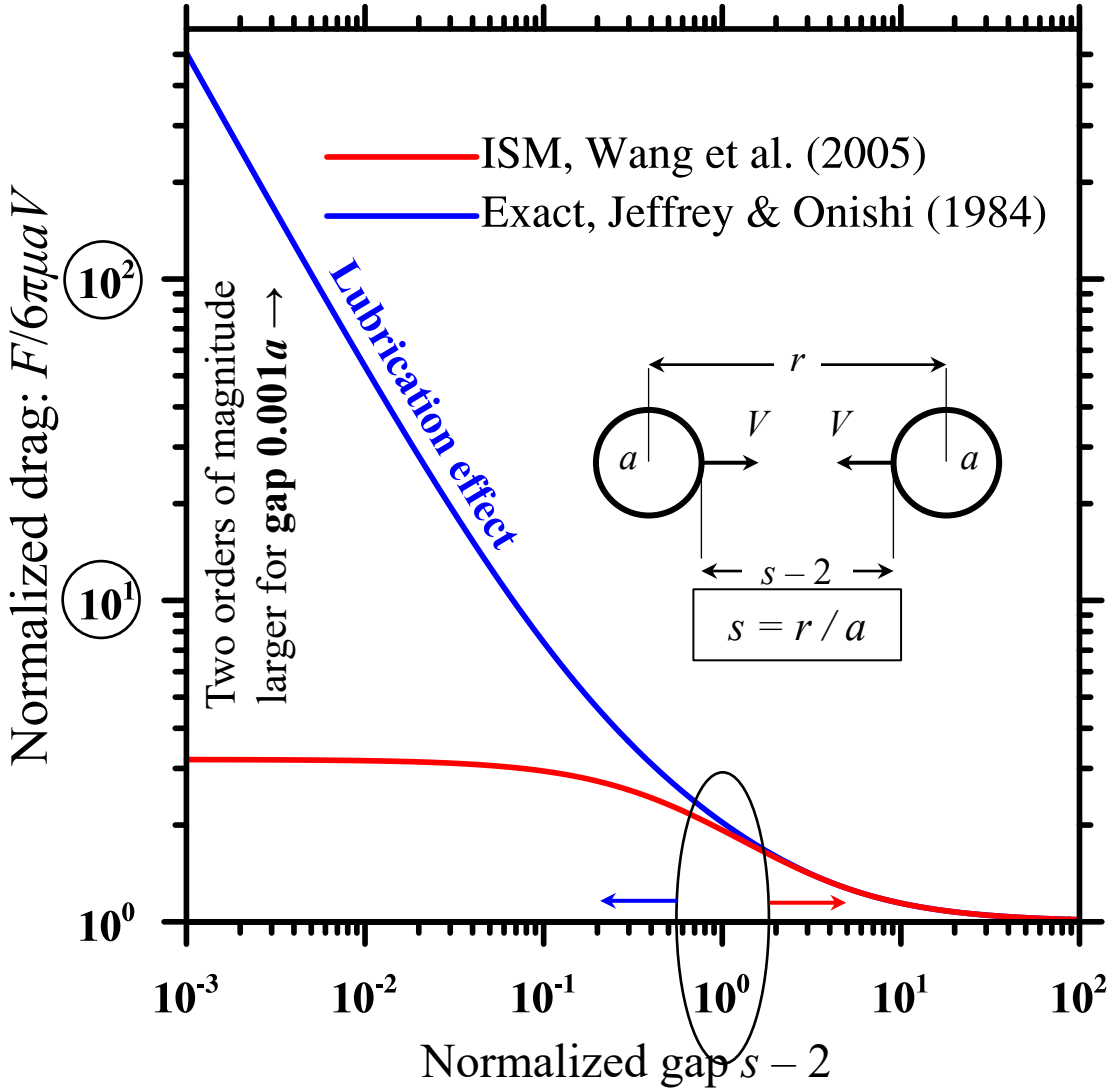

Wang *et al.* (2005):

"While our improved formulations still perform better than the original formulation, all the formulations based on the superposition method fail to predict the lubrication effect."

$a_1 = a_2$ (monodisperse)
Two blue lines

Normalized magnitude of the drag force acting on two same-size spherical particles, whether approaching or receding, along their line of centers as a function of nondimensional gap between their surfaces.

Aerodynamic interactions

Computing AIs from the analytical solutions of Jeffrey & Onishi (1984)

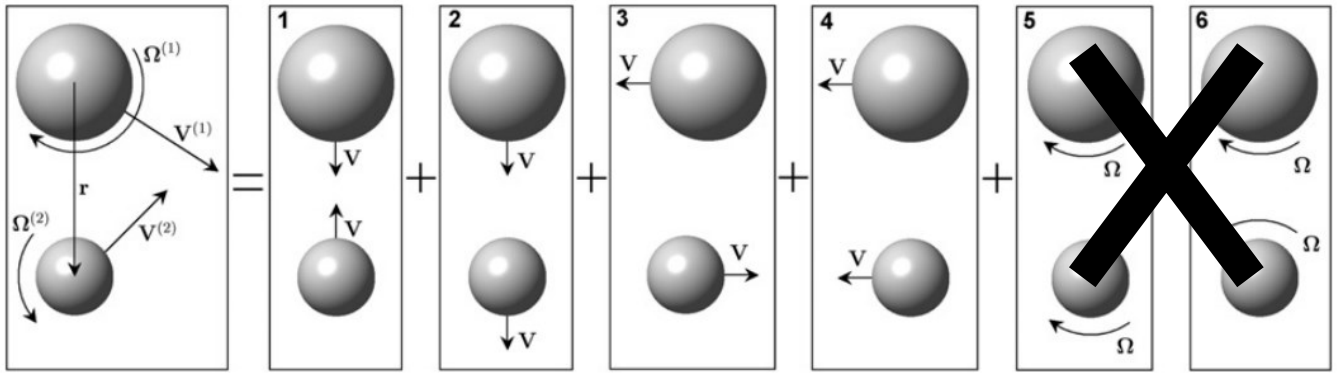

$$\begin{pmatrix} F_1 \\ F_2 \\ L_1 \\ L_2 \end{pmatrix} = \mu \begin{pmatrix} A_{11} & A_{12} & \tilde{B}_{11} & \tilde{B}_{12} \\ A_{21} & A_{22} & \tilde{B}_{21} & \tilde{B}_{22} \\ B_{11} & B_{12} & C_{11} & C_{12} \\ B_{21} & B_{22} & C_{21} & C_{22} \end{pmatrix} \begin{pmatrix} U_1 - U(x_1) \\ U_2 - U(x_2) \\ \Omega_1 - \Omega \\ \Omega_2 - \Omega \end{pmatrix}$$

$$A_{ij}^{(\alpha\beta)} = A_{ji}^{(\beta\alpha)}, \quad \tilde{B}_{ij}^{(\alpha\beta)} = B_{ji}^{(\beta\alpha)}, \quad C_{ij}^{(\alpha\beta)} = C_{ji}^{(\beta\alpha)},$$

Ignore rotational motion

- No rotation considered in ISM (HDNS)
- Considering rotational motion JO solutions is very time-consuming

$$X_{\alpha\beta}^{A}(s,\lambda)$$
$$Y_{\alpha\beta}^{A}(s,\lambda)$$
$$Y_{\alpha\beta}^{B}(s,\lambda)$$
$$X_{\alpha\beta}^{C}(s,\lambda)$$
$$Y_{\alpha\beta}^{C}(s,\lambda)$$

$$s = \frac{2r}{a_1 + a_2}, \quad \lambda = \frac{a_2}{a_1}$$

Aerodynamic interactions

Computing AIs from the analytical solutions of Jeffrey & Onishi (1984)

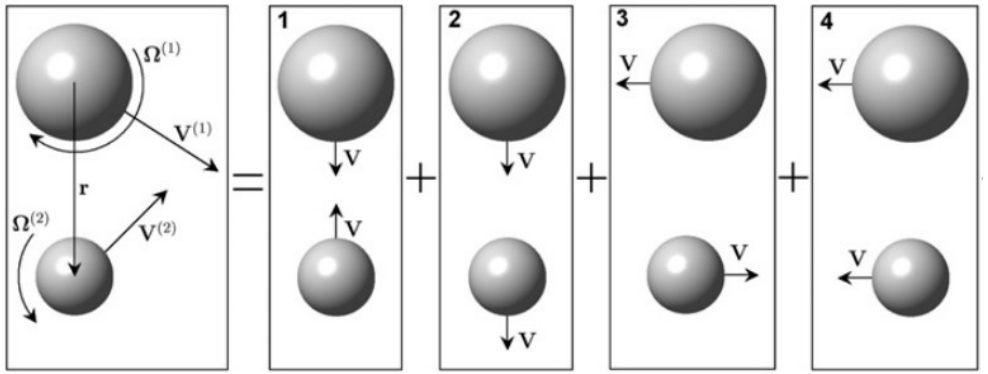

$$\frac{1}{3\pi\mu(a_1+a_2)}\begin{pmatrix}\boldsymbol{F}^{(1)}_{\text{lub}}\\ \boldsymbol{F}^{(2)}_{\text{lub}}\end{pmatrix}=\begin{pmatrix}\boldsymbol{u}^{(1)}_{\text{lub}}\\ \boldsymbol{u}^{(2)}_{\text{lub}}\end{pmatrix}=\begin{bmatrix}\boldsymbol{A}_{11} & \boldsymbol{A}_{12}\\ \boldsymbol{A}_{21} & \boldsymbol{A}_{22}\end{bmatrix}\begin{pmatrix}\boldsymbol{V}^{(1)}-\boldsymbol{U}^{(1)}\\ \boldsymbol{V}^{(2)}-\boldsymbol{U}^{(2)}\end{pmatrix},$$

$$\boldsymbol{A}_{\alpha\beta}\,\boldsymbol{v}^{(\beta)}=X^{\boldsymbol{A}}_{\alpha\beta}\frac{\boldsymbol{r}}{r^2}\left(\boldsymbol{r}\cdot\boldsymbol{v}^{(\beta)}\right)+Y^{\boldsymbol{A}}_{\alpha\beta}\left(\boldsymbol{v}^{(\beta)}-\frac{\boldsymbol{r}}{r^2}\left(\boldsymbol{r}\cdot\boldsymbol{v}^{(\beta)}\right)\right),$$

$$X^{A}_{11}=g_1(1-4s^{-2})^{-1}-g_2\ln(1-4s^{-2})-g_3(1-4s^{-2})\ln(1-4s^{-2})+f_0(\lambda)-g_1$$
$$+\sum_{\substack{m=2\\ m\text{ even}}}^{\infty}\{2^{-m}(1+\lambda)^{-m}f_m(\lambda)-g_1-2m^{-1}g_2+4m^{-1}m_1^{-1}g_3\}\left(\frac{2}{s}\right)^m,$$

where $$m_1=-2\delta_{m2}+(m-2)(1-\delta_{m2});$$

$$-\tfrac{1}{2}(1+\lambda)X^{A}_{12}=2s^{-1}g_1(1-4s^{-2})^{-1}+g_2\ln\frac{s+2}{s-2}+g_3(1-4s^{-2})\ln\frac{s+2}{s-2}+4g_3\,s^{-1}$$
$$+\sum_{\substack{m=1\\ m\text{ odd}}}^{\infty}\{2^{-m}(1+\lambda)^{-m}f_m(\lambda)-g_1-2m^{-1}g_2+4m^{-1}m_1^{-1}g_3\}\left(\frac{2}{s}\right)^m.$$

$$g_1=2\lambda^2(1+\lambda)^{-3},\quad g_2=\tfrac{1}{5}\lambda(1+7\lambda+\lambda^2)(1+\lambda)^{-3},$$
$$g_3=\tfrac{1}{42}(1+18\lambda-29\lambda^2+18\lambda^3+\lambda^4)(1+\lambda)^{-3}.$$

$$f_k(\lambda)=2^k\sum_{q=0}^{k}P_{1(k-q)\,q}\,\lambda^q.$$

$$P_{n00}=V_{n00}=\delta_{1n},$$

$$V_{npq}=P_{npq}-\frac{2n}{(n+1)(2n+3)}\sum_{s=1}^{q}\binom{n+s}{n}P_{s(q-s)(p-n-1)},$$

$$P_{npq}=\sum_{s=1}^{q}\binom{n+s}{n}\left[\frac{n(2n+1)(2ns-n-s+2)}{2(n+1)(2s-1)(n+s)}P_{s(q-s)(p-n+1)}\right.$$
$$\left.-\frac{n(2n-1)}{2(n+1)}P_{s(q-s)(p-n-1)}-\frac{n(4n^2-1)}{2(n+1)(2s+1)}V_{s(q-s-2)(p-n+1)}\right].$$

Aerodynamic interactions

Coupled implementation of HDNS and analytical solutions of JO84

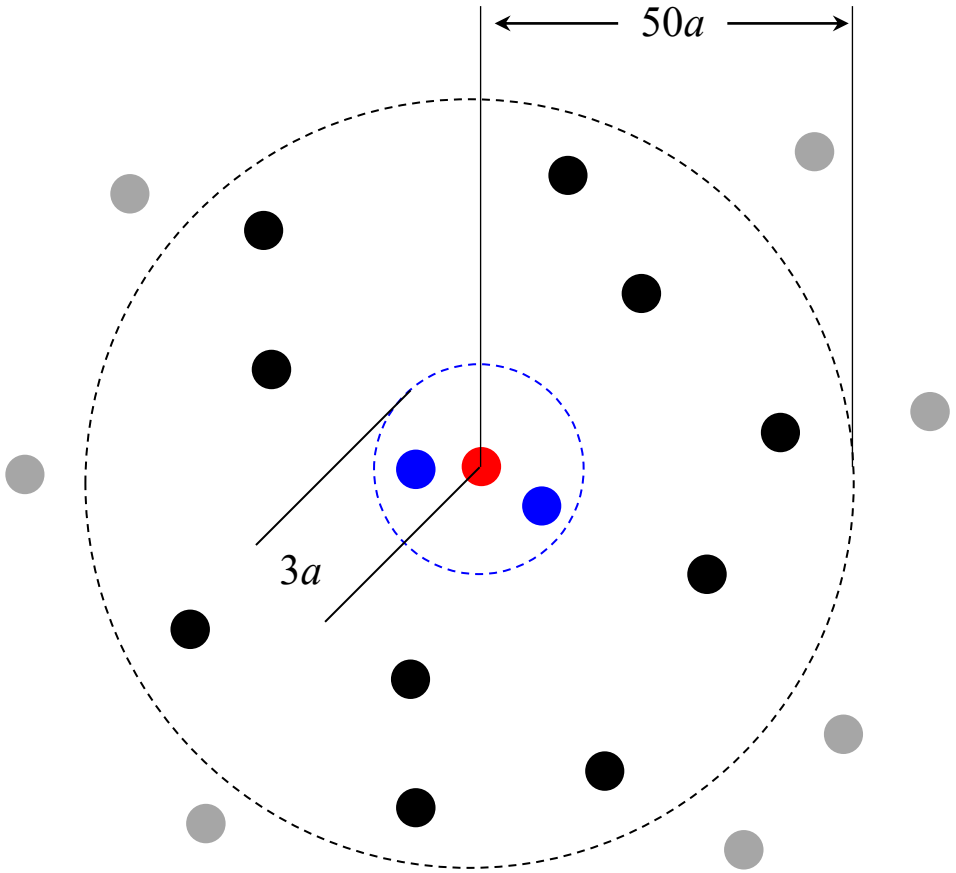

The interaction regions (spheres) around each droplet:

- red: particle of consideration;
- blue: particles with $r < 3a$ to the particle of consideration;
- black: particles with distances $3a < r < 50a$;
- grey: distant particles $r > 50a$.

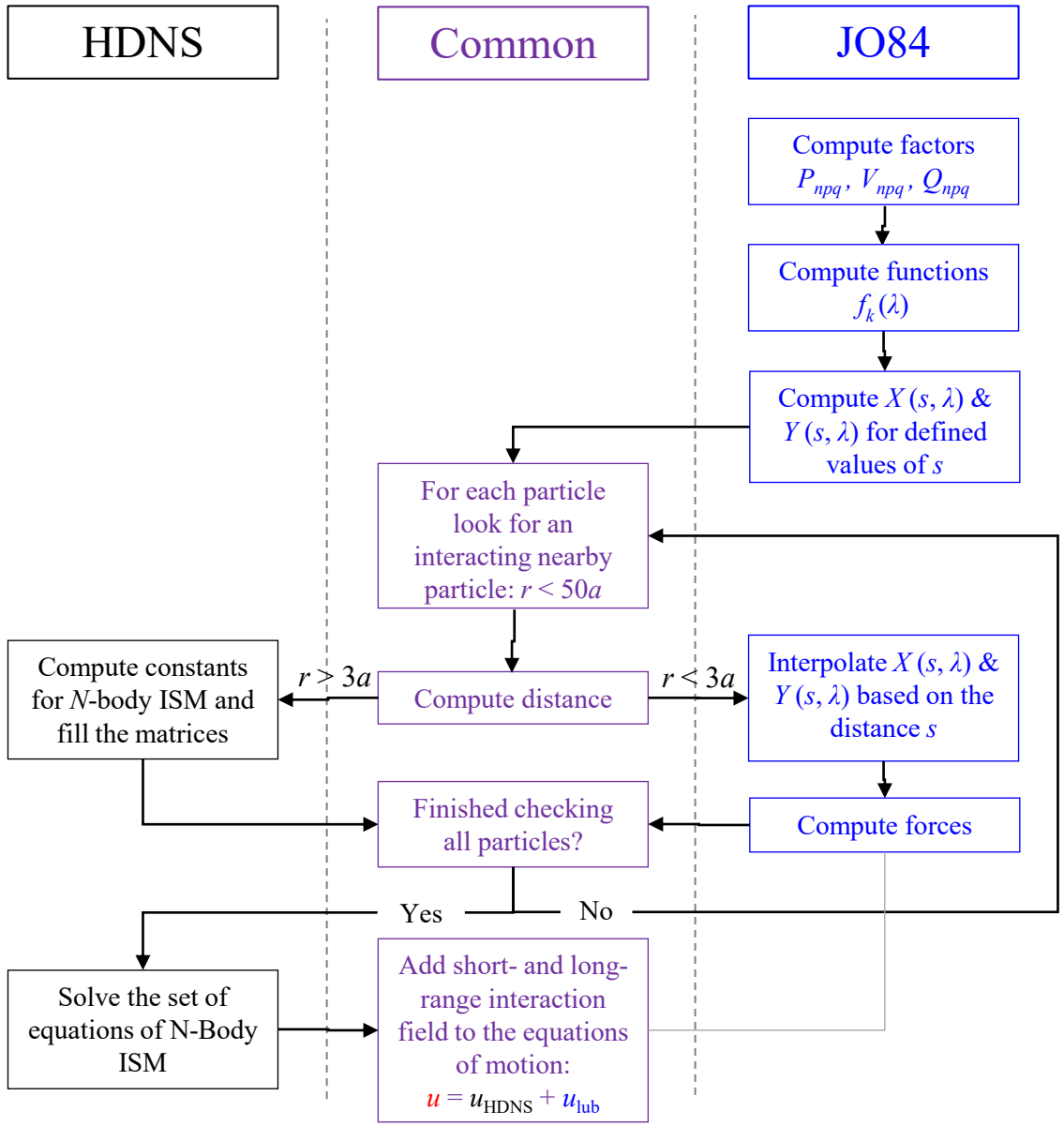

Collision statistics

RDF, RRV, kinematic and dynamic collision kernels: $g_r(r/R)$, $\langle|w_r(r/R)|\rangle$, Γ^{K} and Γ^{D}

1. Introduce the particles
2. Evolve the system for $10T_{\mathrm{e}}$ (statistically stationary)
3. Start collecting samples from the following:

Collision sphere radius: $R = a_1 + a_2 = 2a$

Radial distribution function (RDF): $$g_r\left(\frac{r}{R};t\right) = \frac{n_{\mathrm{pair}}\left(r/R;t\right)/V_{\mathrm{shell}}\left(r/R\right)}{\frac{1}{2}N_{\mathrm{p}}\left(N_{\mathrm{p}}-1\right)/V_{\mathrm{box}}}$$

→ Measure of clustering
$g_r = 1$: uniform distribution
$g_r > 1$: clustering

Radial relative velocity (RRV): $$\left\langle\left|w_r\left(\frac{r}{R};t\right)\right|\right\rangle = \frac{\sum_{n=1}^{n_{\mathrm{pair}}}\left|\boldsymbol{V}^{(k)}-\boldsymbol{V}^{(n)}\right|\cdot\boldsymbol{r}/r}{n_{\mathrm{pair}}\left(r/R;t\right)}$$

Kinematic collision kernel: $$\Gamma^{\mathrm{K}} = 2\pi R^2\left\langle\left|w_r\left(r=R\right)\right|\right\rangle g_r\left(r=R\right)$$

→ Volumetric rate of collision

Dynamic collision kernel: $$\Gamma^{\mathrm{D}} = \frac{\dot{N}_{\mathrm{c}} \;\rightarrow \text{Rate of collision}}{\frac{1}{2}N_{\mathrm{p}}\left(N_{\mathrm{p}}-1\right)/V_{\mathrm{box}}}$$

Results

Sensitivity of droplet collision statistics to time step size

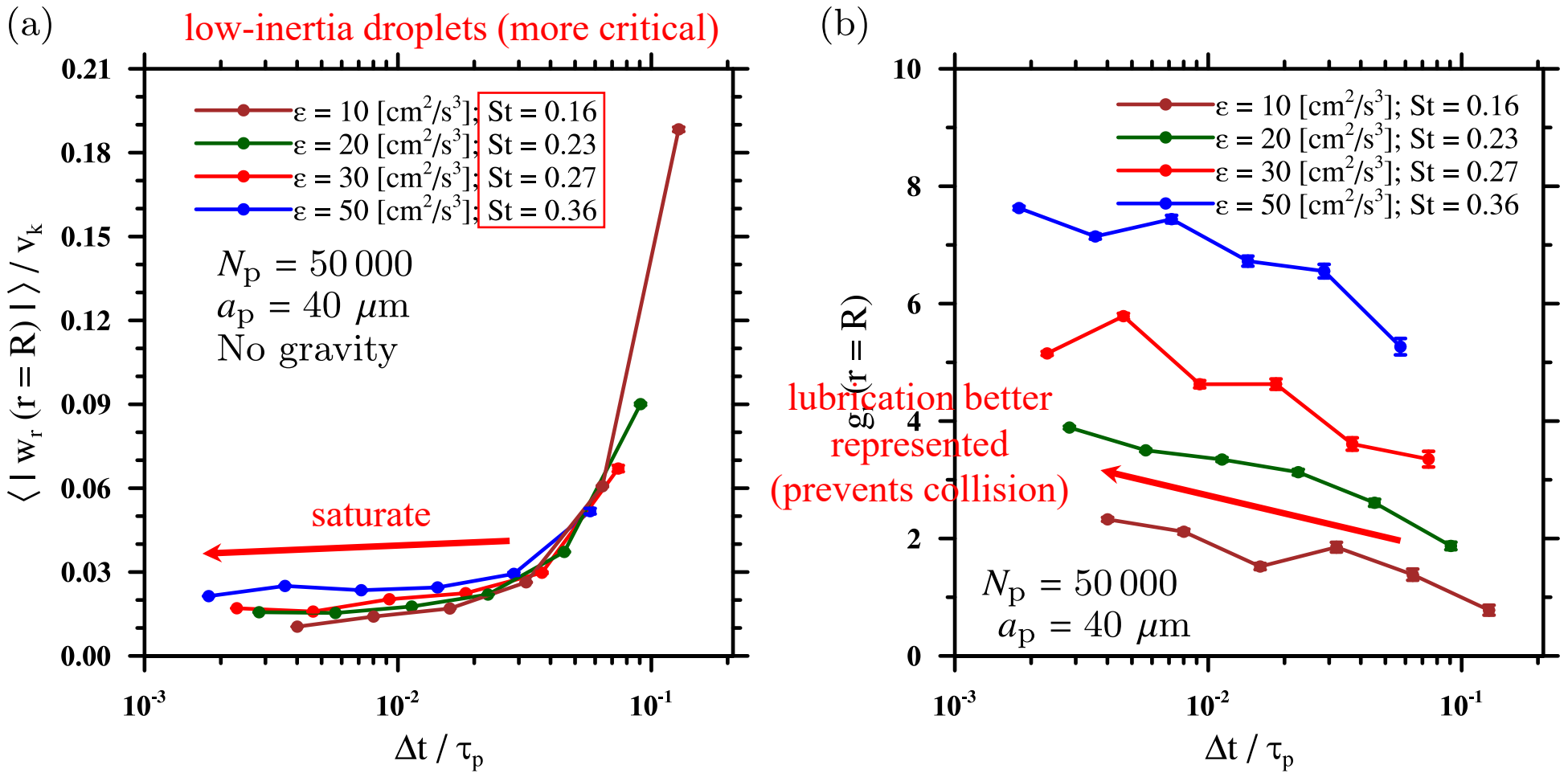

Two-point collision statistics at contact computed using different time steps:
(a) normalized radial relative velocity and (b) radial distribution function.

Results

Sensitivity of droplet collision statistics to time step size

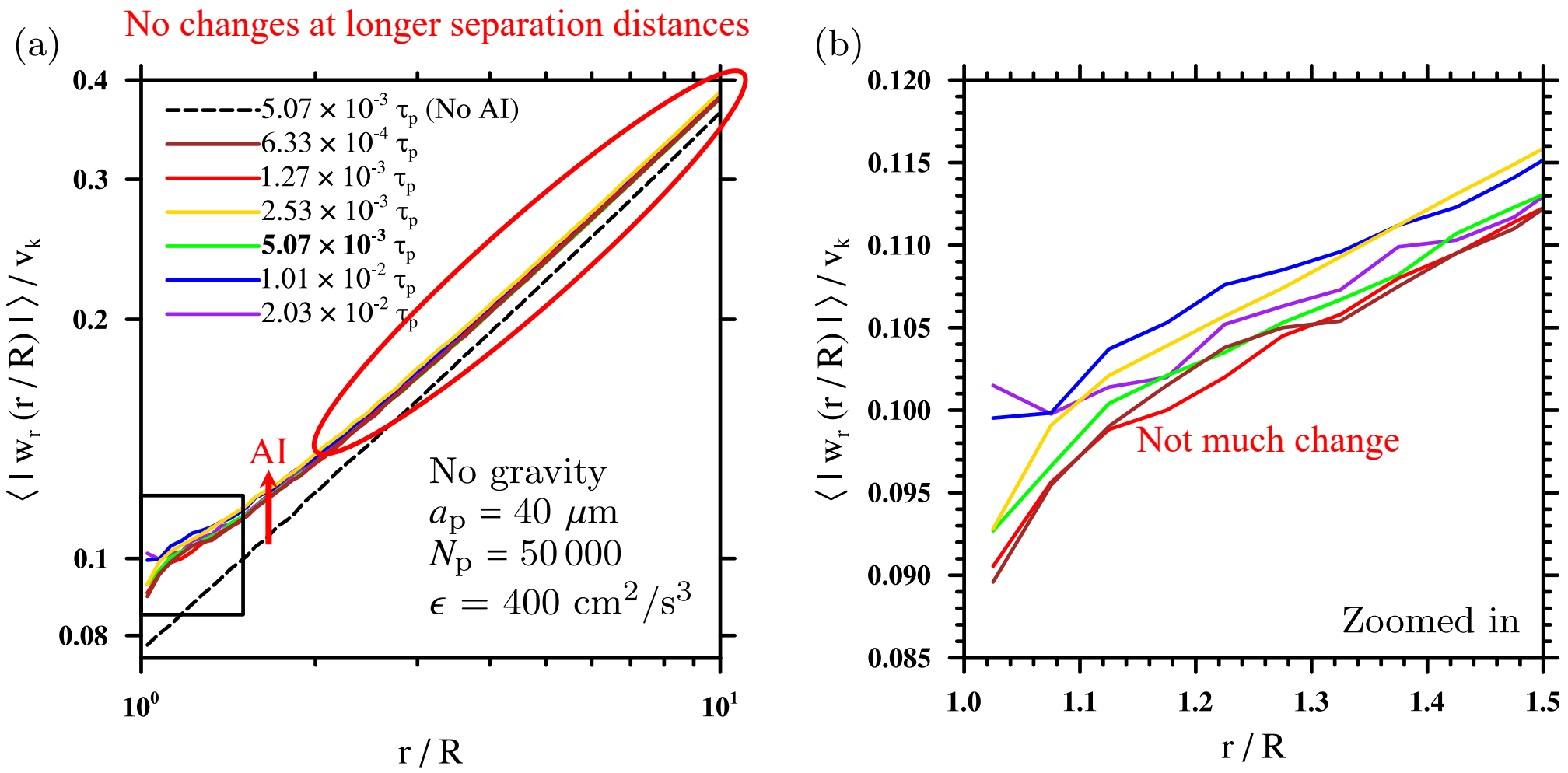

RRV computed using different time step sizes for the normalized separation distance in the range: (a) $1 < r / R < 10$ and (b) $1 < r / R < 1.5$ with the set of droplets $a_p = 40$ μm and $N_p = 50\,000$. The black rectangle in (a) marks the region that is enlarged and shown in (b).

Results

Sensitivity of droplet collision statistics to time step size

Overall conclusion: compromise between accuracy and simulation time because $\Delta t\downarrow$ then evolution time$\downarrow$ hence uncertainty$\uparrow$

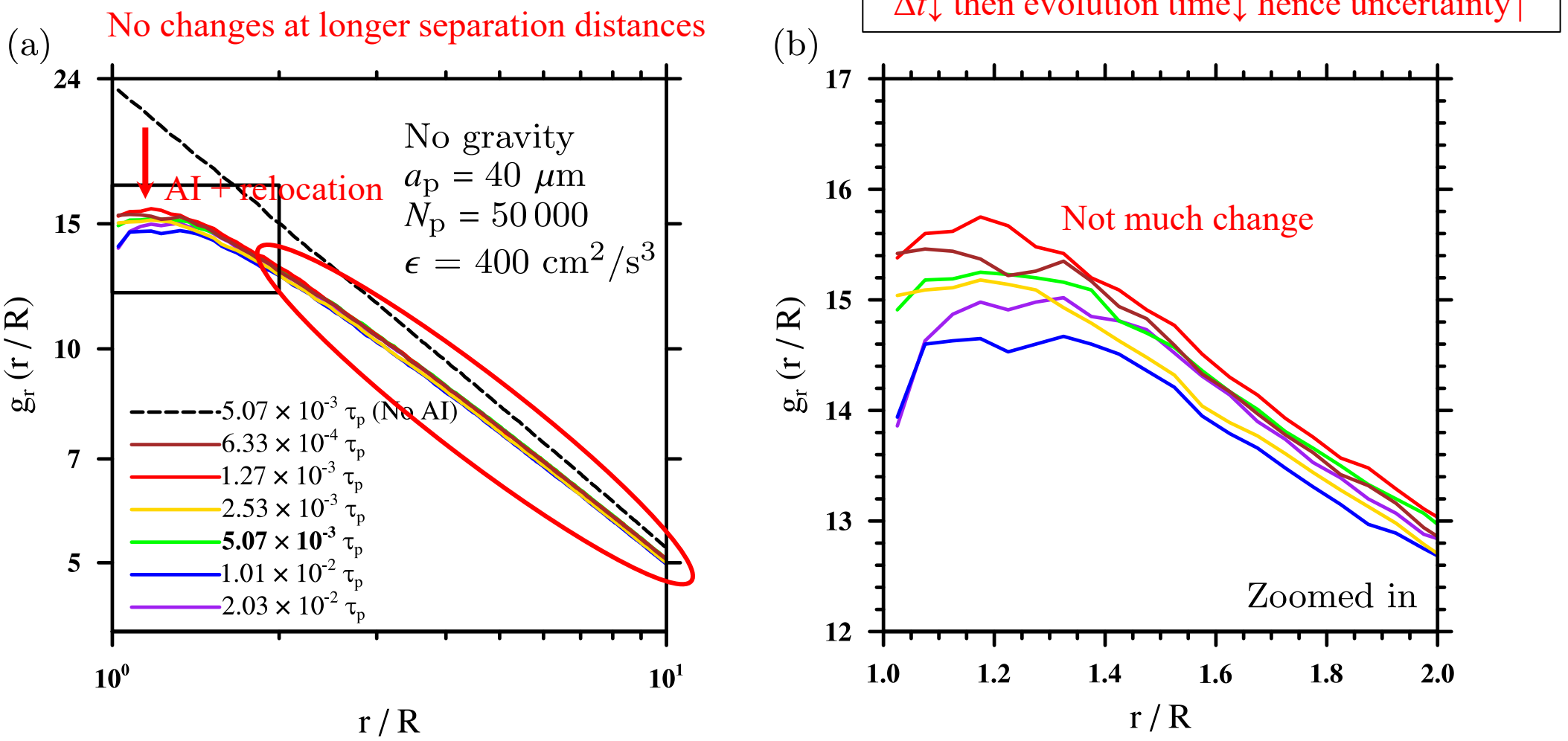

RDF computed using different time step sizes for the normalized separation distance in the range: (a) $1 < r / R < 10$ and (b) $1 < r / R < 2$ with the set of droplets a_p = 40 μm and N_p = 50 000. The black rectangle in (a) marks the region that is enlarged and shown in (b).

Results

Sensitivity of droplet collision statistics to time step size

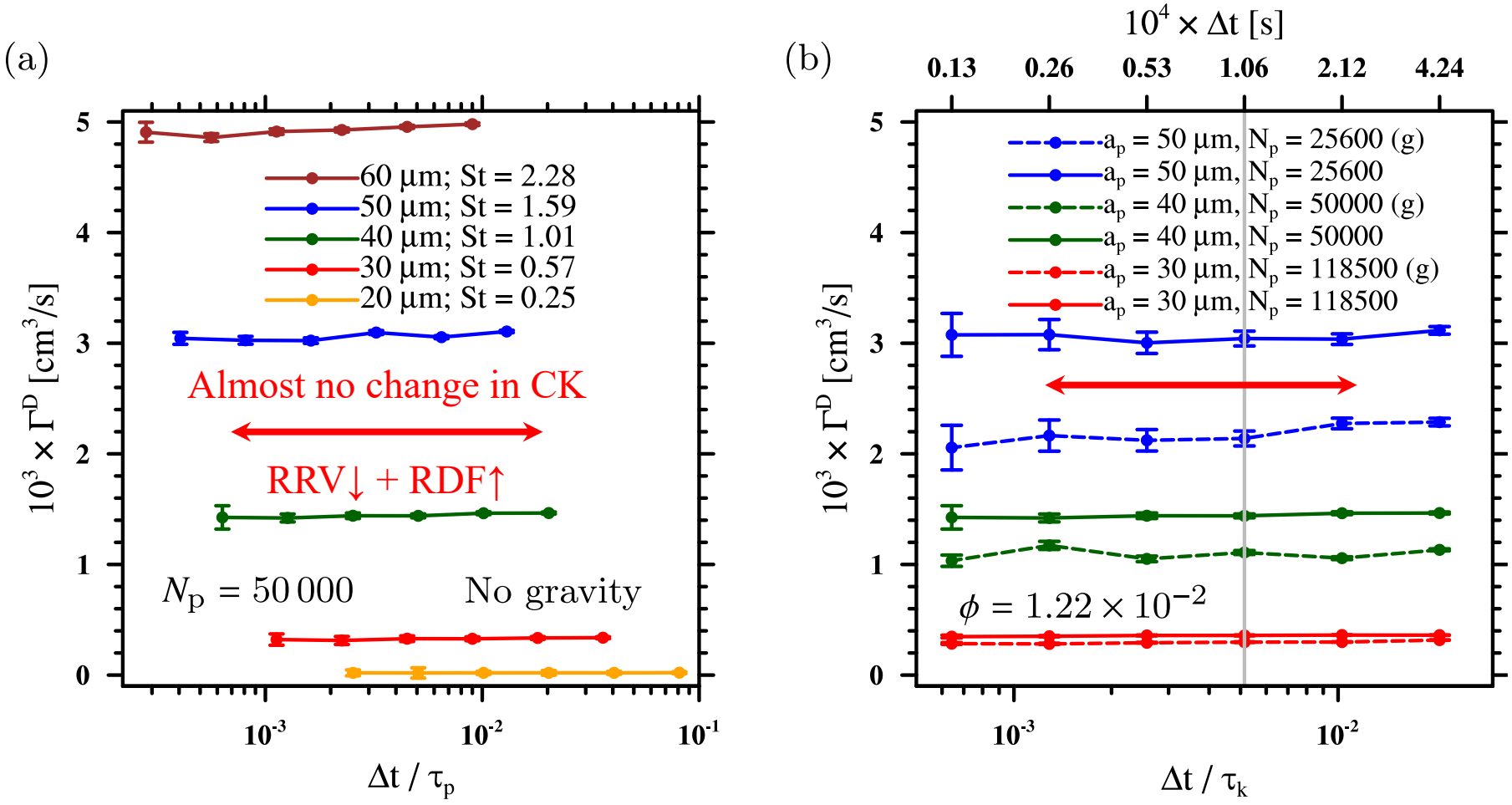

The effect of time step size on the dynamic collision kernel for (a) the same number of droplets: N_p = 50 000 and (b) the same mass loading: $\varphi = 1.22 \times 10^{-2}$, considering various sets of same-size droplets with different radii.

Results

Setting an optimal location for the matching point δ

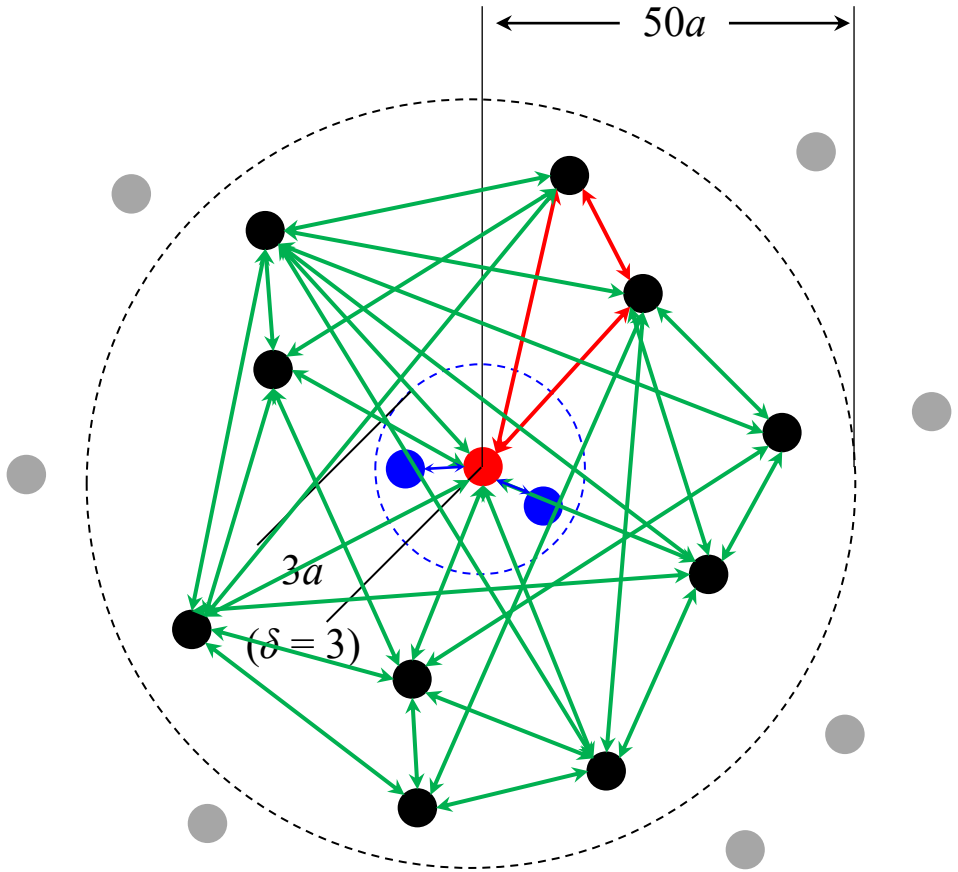

HDNS handles many-body interaction

JO solutions capture lubrication effects

Variations in the radial relative velocity for the sets of droplets (a) a_p = 40 μm; N_p = 50 000, and (b) a_p = 30 μm; N_p = 118 500 when the lubrication forces are considered within different ranges of interaction δ.

Results

Setting an optimal location for the matching point δ

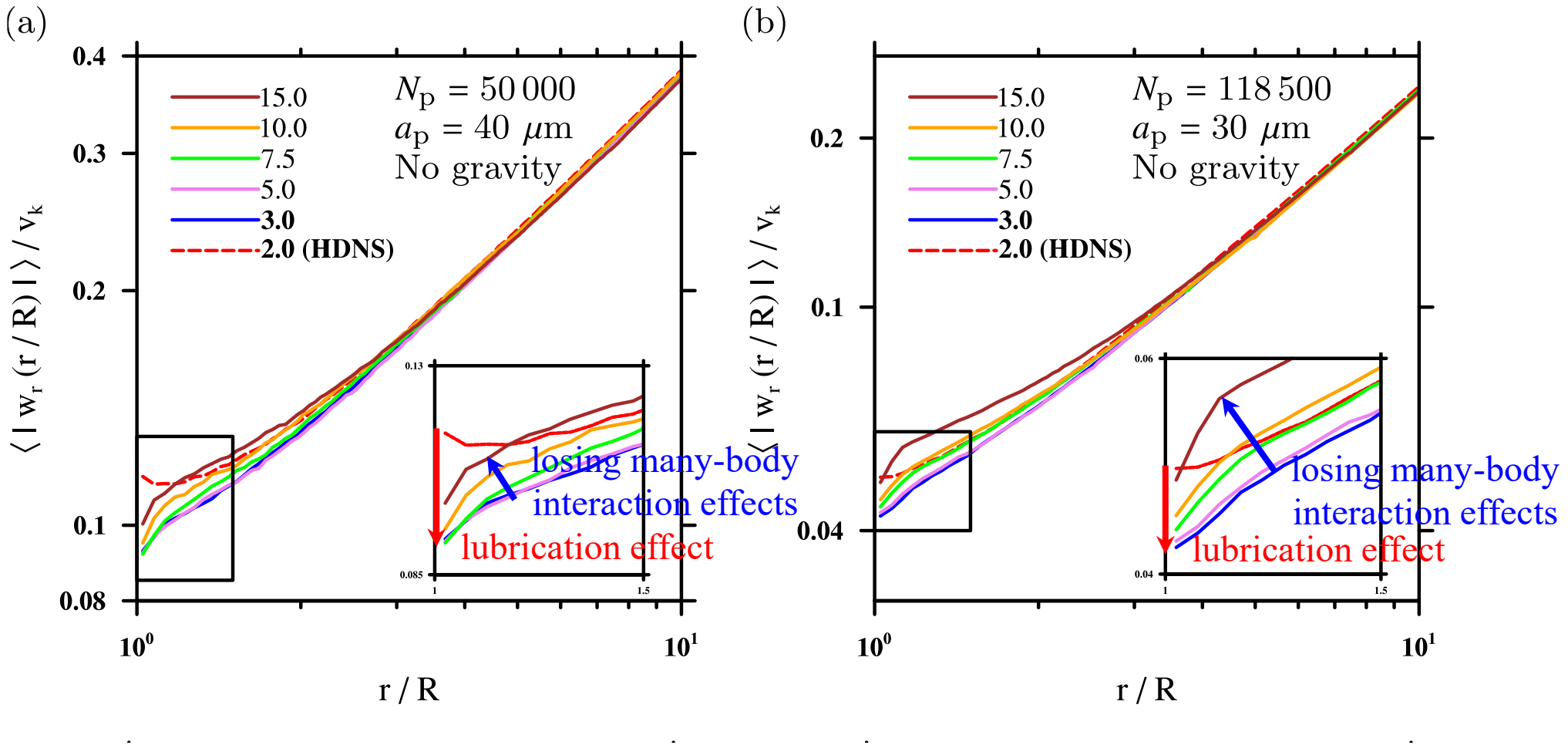

Variations in the radial relative velocity for the sets of droplets (a) a_p = 40 µm; N_p = 50 000, and (b) a_p = 30 µm; N_p = 118 500 when the lubrication forces are considered within different ranges of interaction δ.

Results

Setting an optimal location for the matching point δ

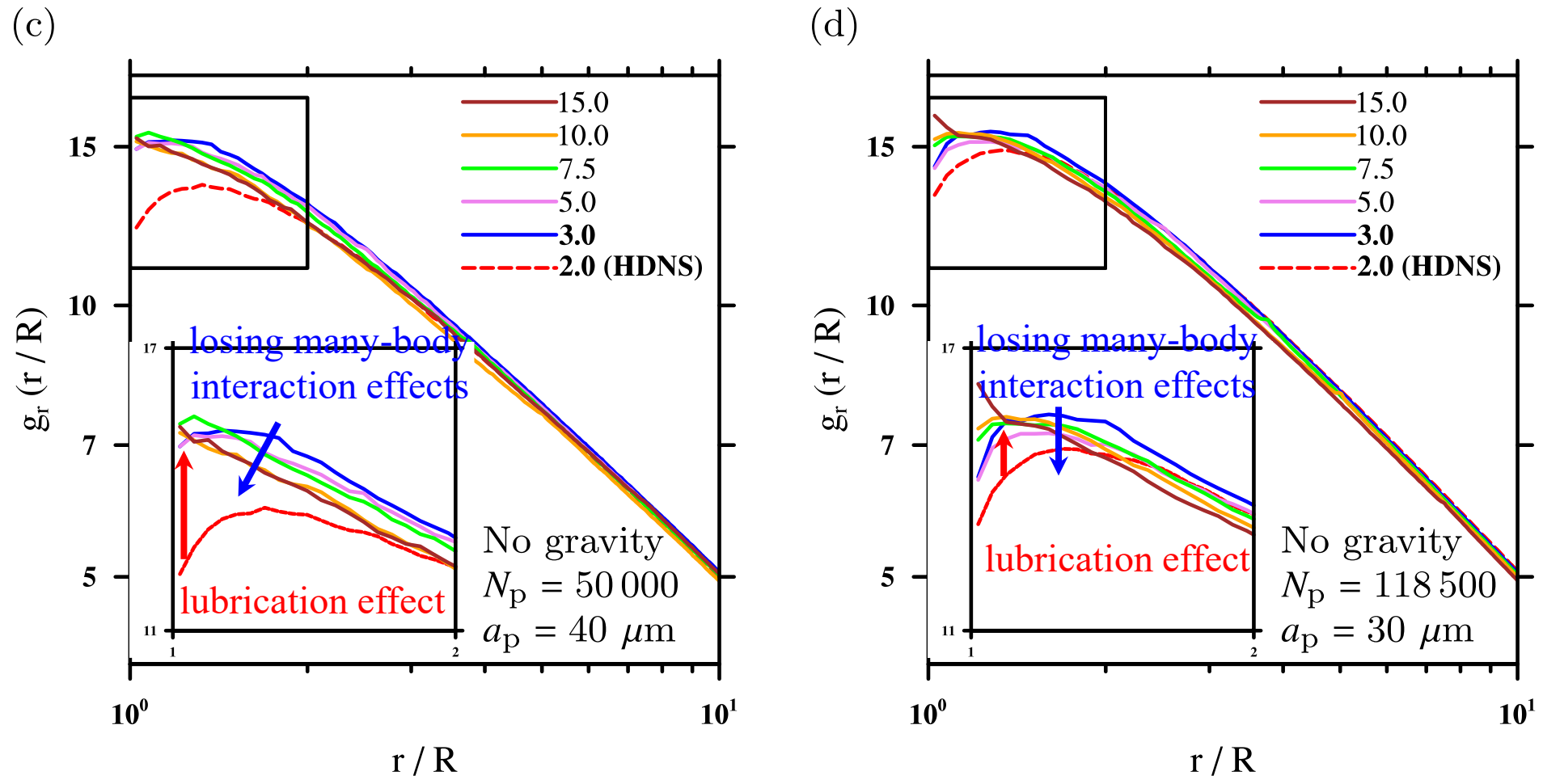

Variations in the radial distribution function for the sets of droplets (c) a_p = 40 μm; N_p = 50 000, and (d) a_p = 30 μm; N_p = 118 500 when the lubrication forces are considered within different ranges of interaction δ.

Results

Setting an optimal location for the matching point δ

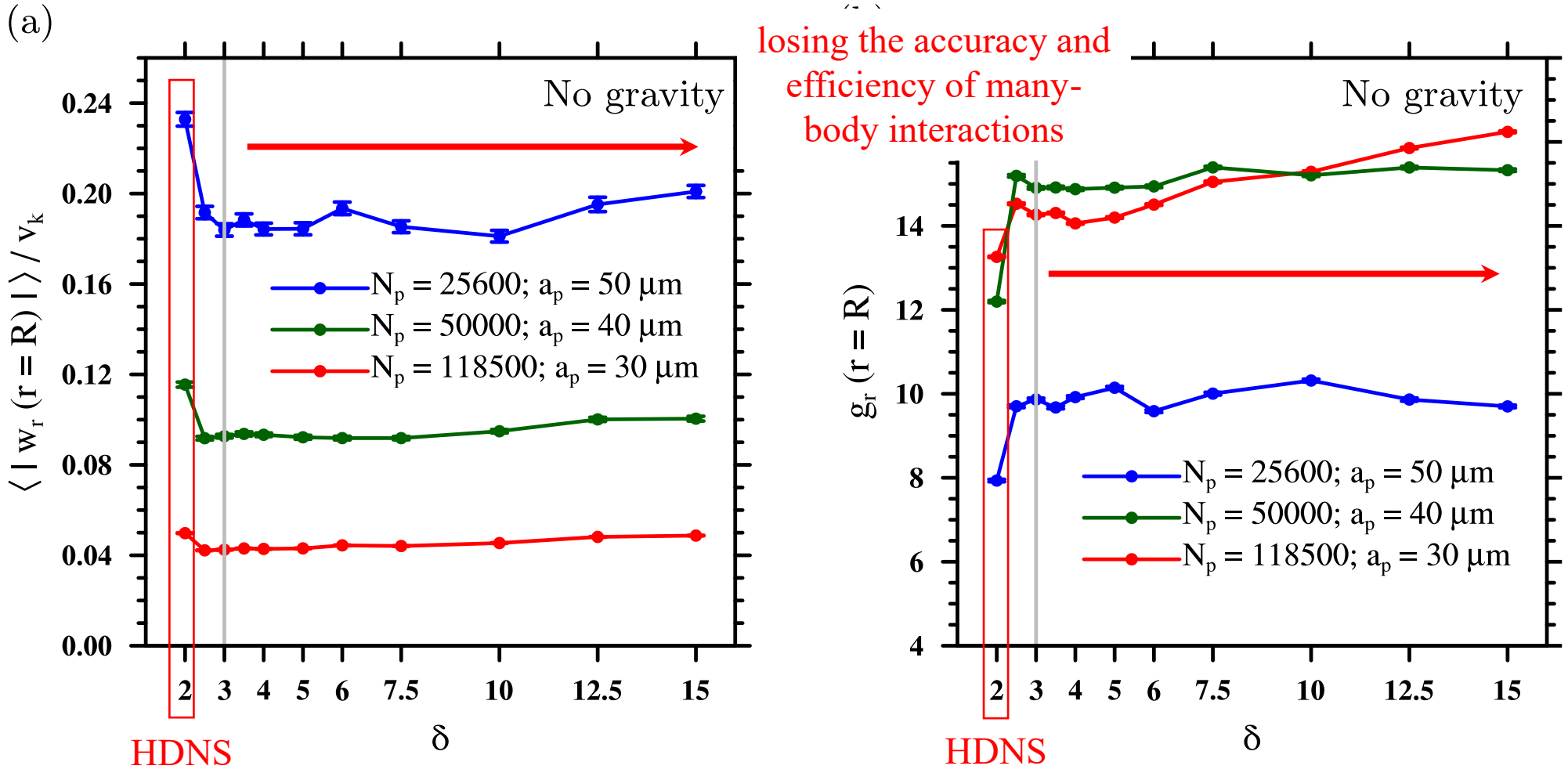

Variations in the (a) at-contact radial relative velocity and (b) at-contact radial distribution function for three sets of droplets with the same mass loading, $\varphi = 1.22\times10^{-2}$, when the lubrication forces are considered within different ranges of interaction.

Results

Setting an optimal location for the matching point δ

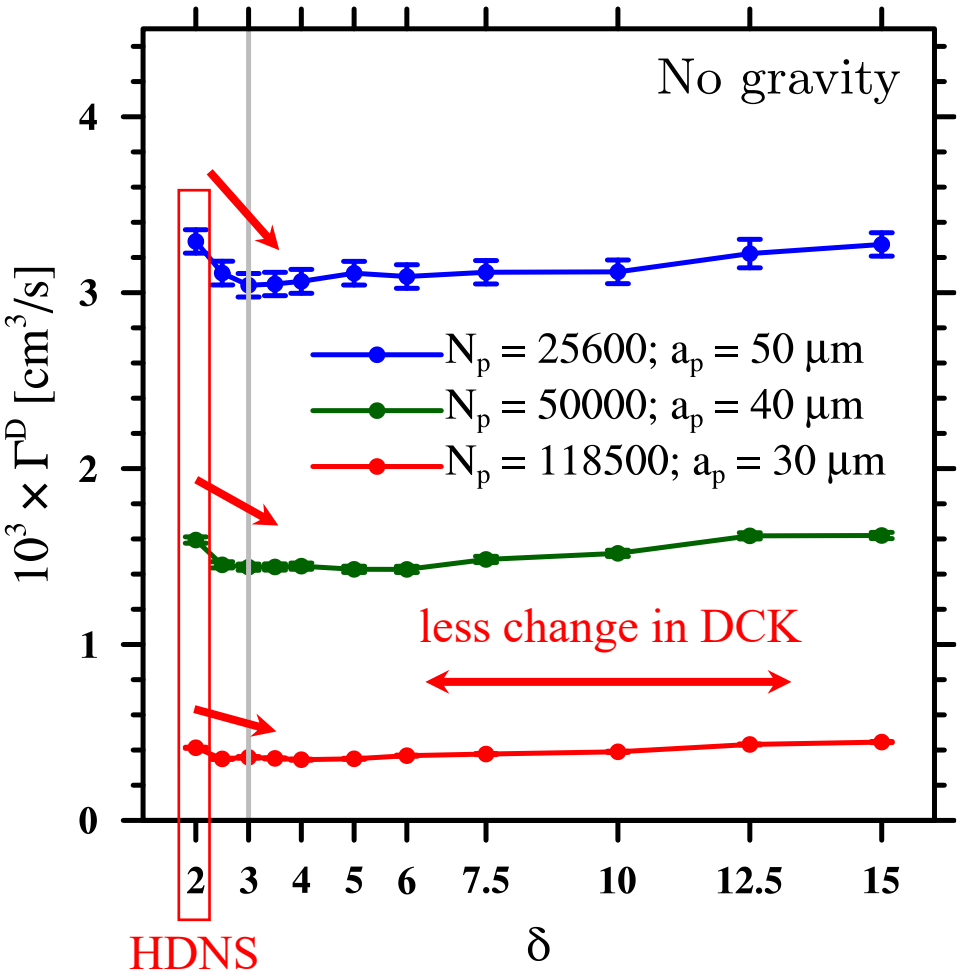

Variations in the dynamic collision kernel for three sets of droplets with the same mass loading, $\varphi = 1.22\times10^{-2}$, when the lubrication forces are considered within different ranges of interaction.

Results

Effects of AIs on kinematic and dynamic collision statistics

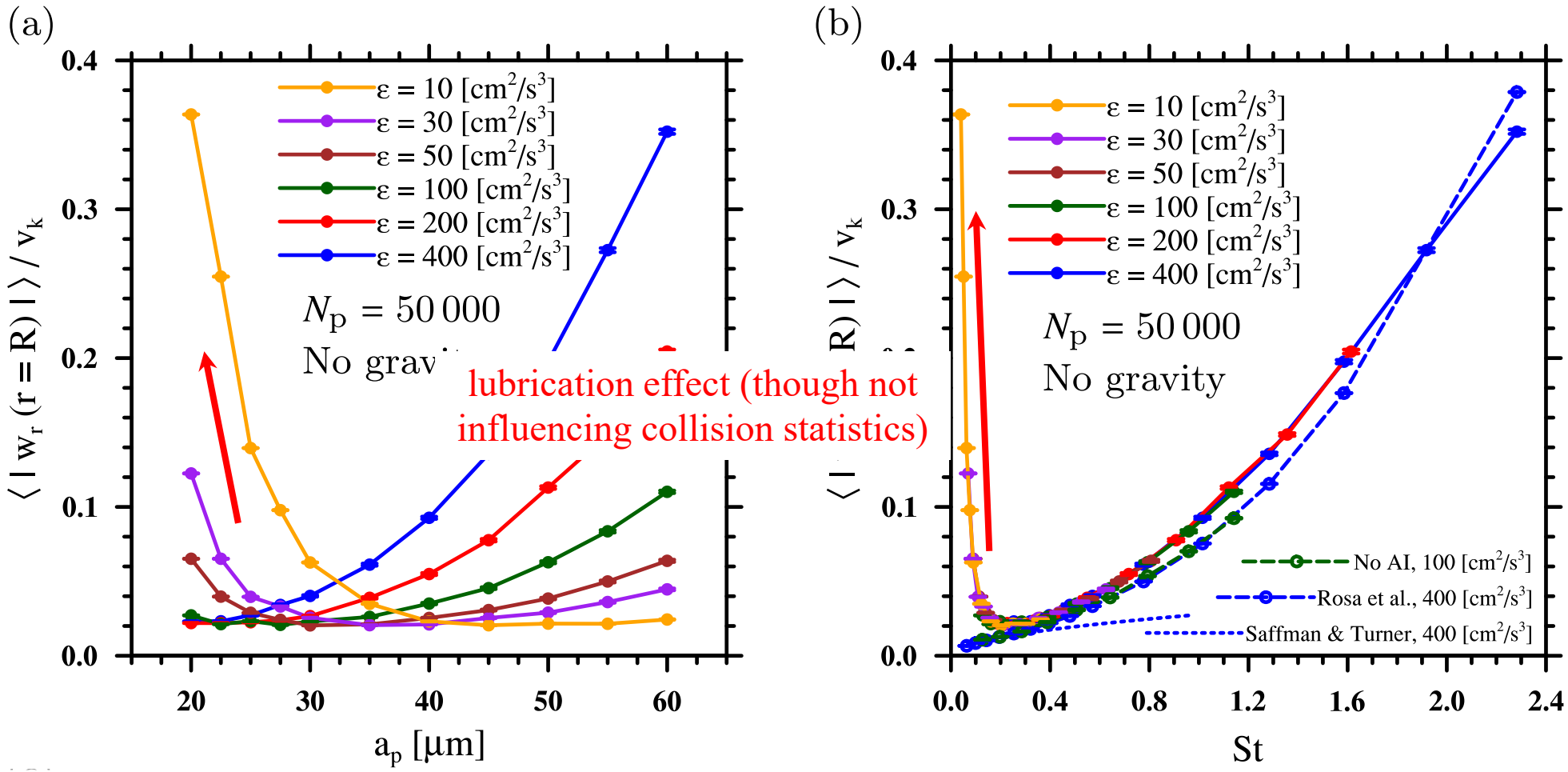

The effect of turbulent energy dissipation rate on the at-contact RRV for different (a) droplet sizes and (b) Stokes numbers. In panel (b) the theoretical model of Saffman & Turner (1956) is shown. The DNS results of Rosa *et al.* (2013, figures 8a and 13a there) are additionally included in panels (b).

Results

Effects of AIs on kinematic and dynamic collision statistics

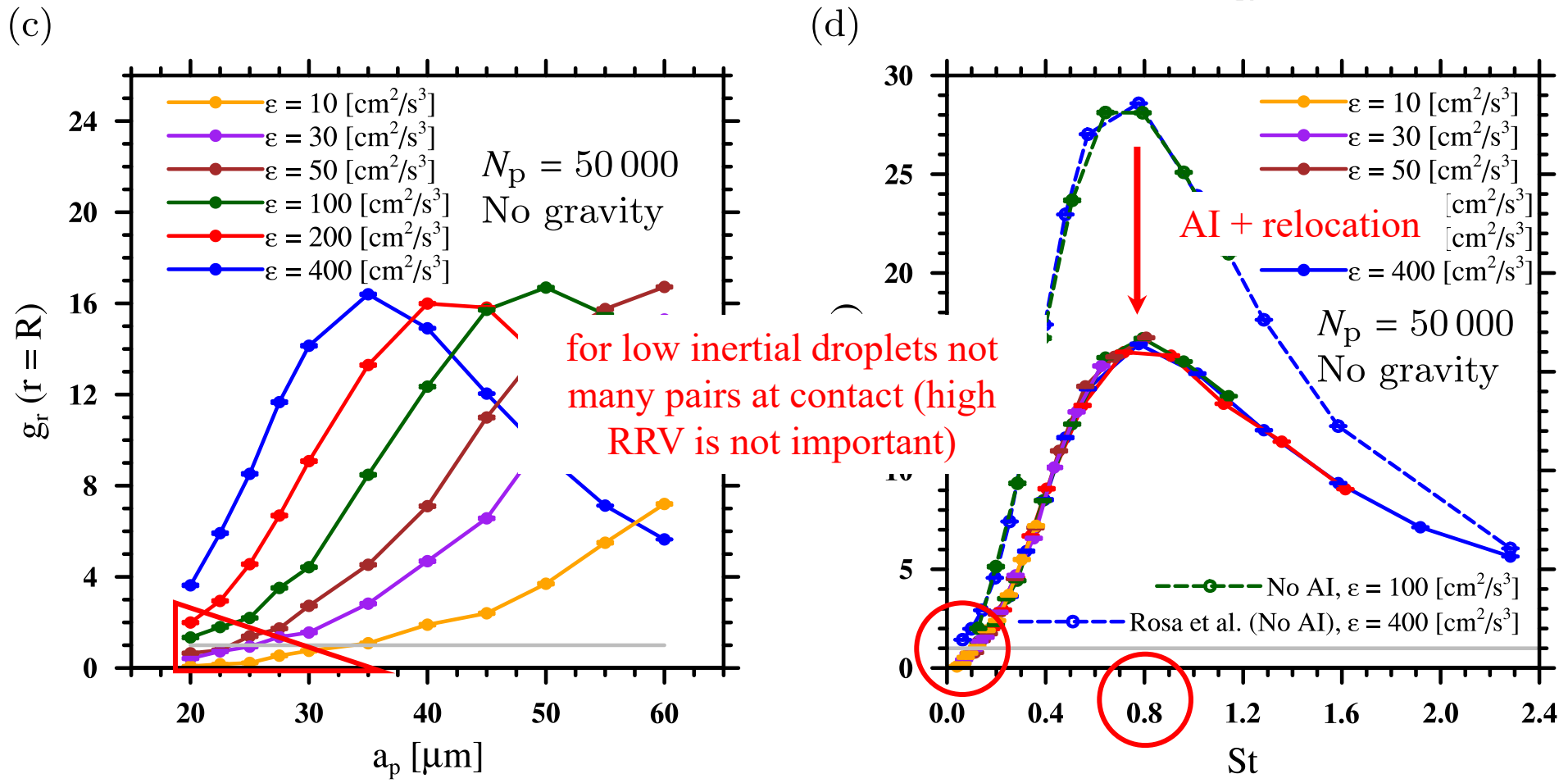

The effect of turbulent energy dissipation rate on the at-contact RDF for different (c) droplet sizes and (d) Stokes numbers. The DNS results of Rosa *et al.* (2013, figures 8a and 13a there) are additionally included in panels (d).

Results

Effects of AIs on kinematic and dynamic collision statistics

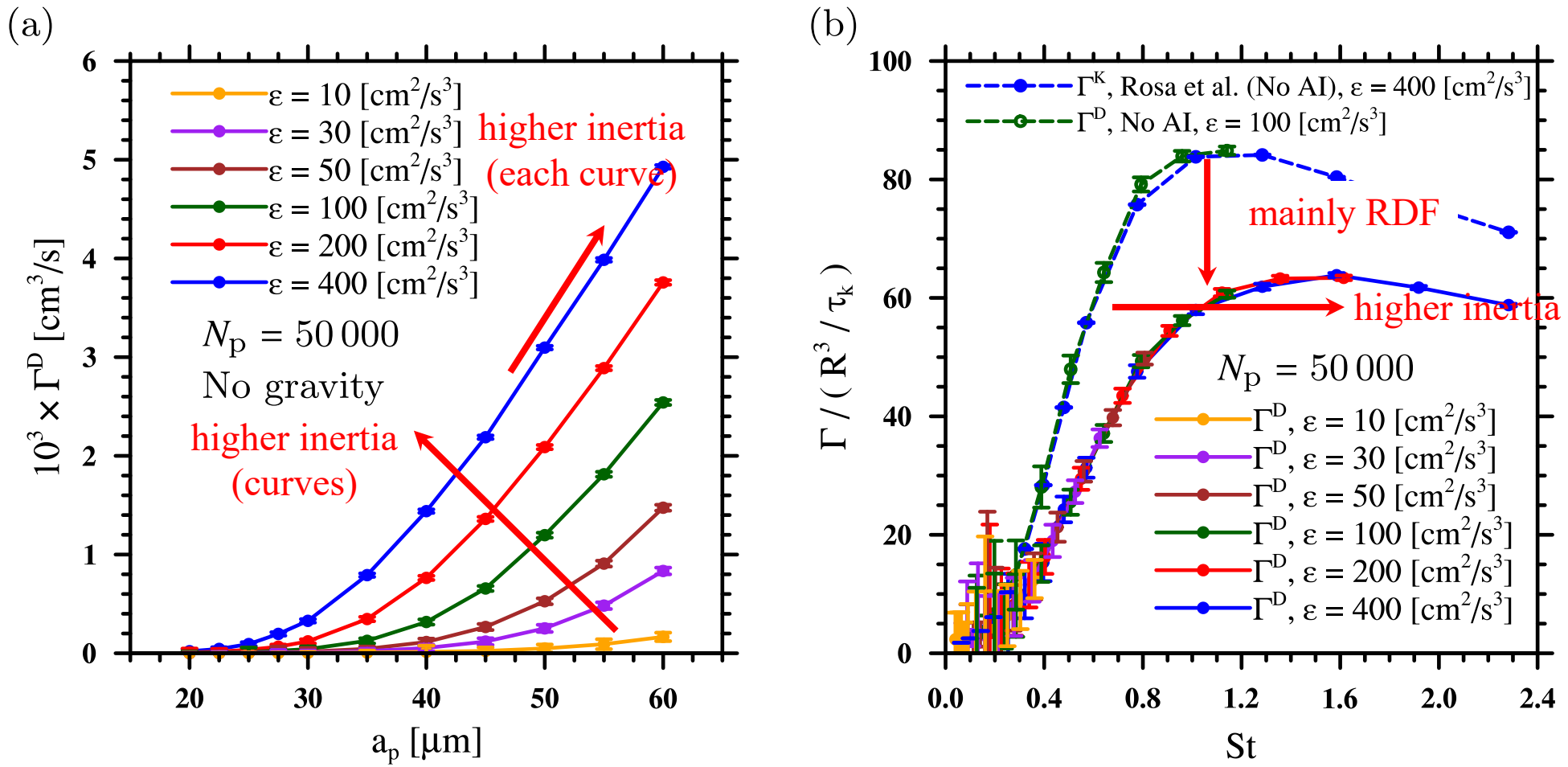

The dynamic collision kernel as function of (a) droplet size in flows with different energy dissipation rates for N_p = 50 000, and (b) the normalized dynamic collision kernel for corresponding values of the Stokes number. The results of Rosa *et al.* (2013) are added to panel (b) for comparison.

Results

Comparison of the new *lubrication-included HDNS* with *standard HDNS* and simulations *without AIs*

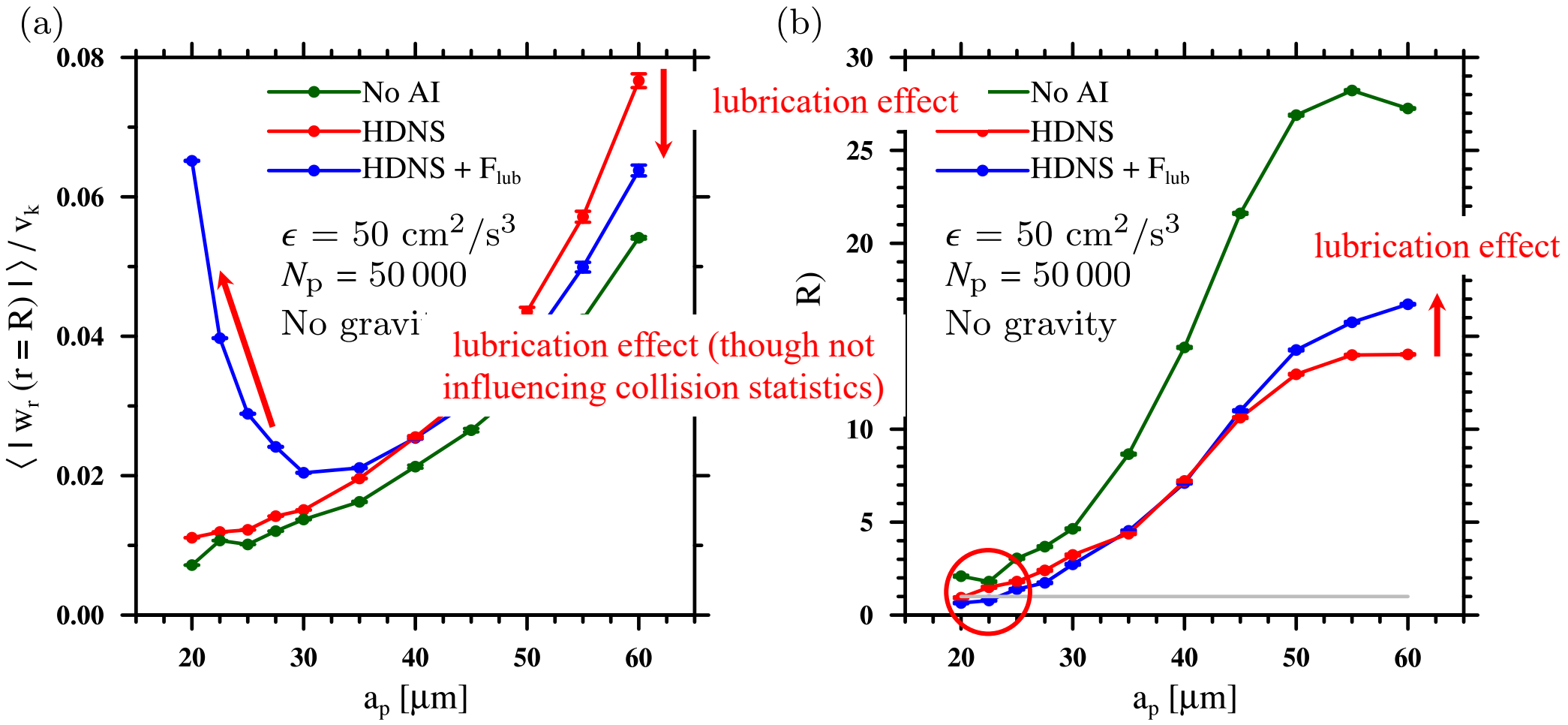

Changes in the at-contact (a) RRVs and (b) RDFs when the effect of lubrication forces is taken into consideration compared with the standard HDNS without lubrication effects as well as the case without aerodynamic interaction for N_p = 50 000 droplets in a flow at a low dissipation rate ε = 50 cm^2/s^3.

Results

Comparison of the new *lubrication-included HDNS* with *standard HDNS* and simulations *without AIs*

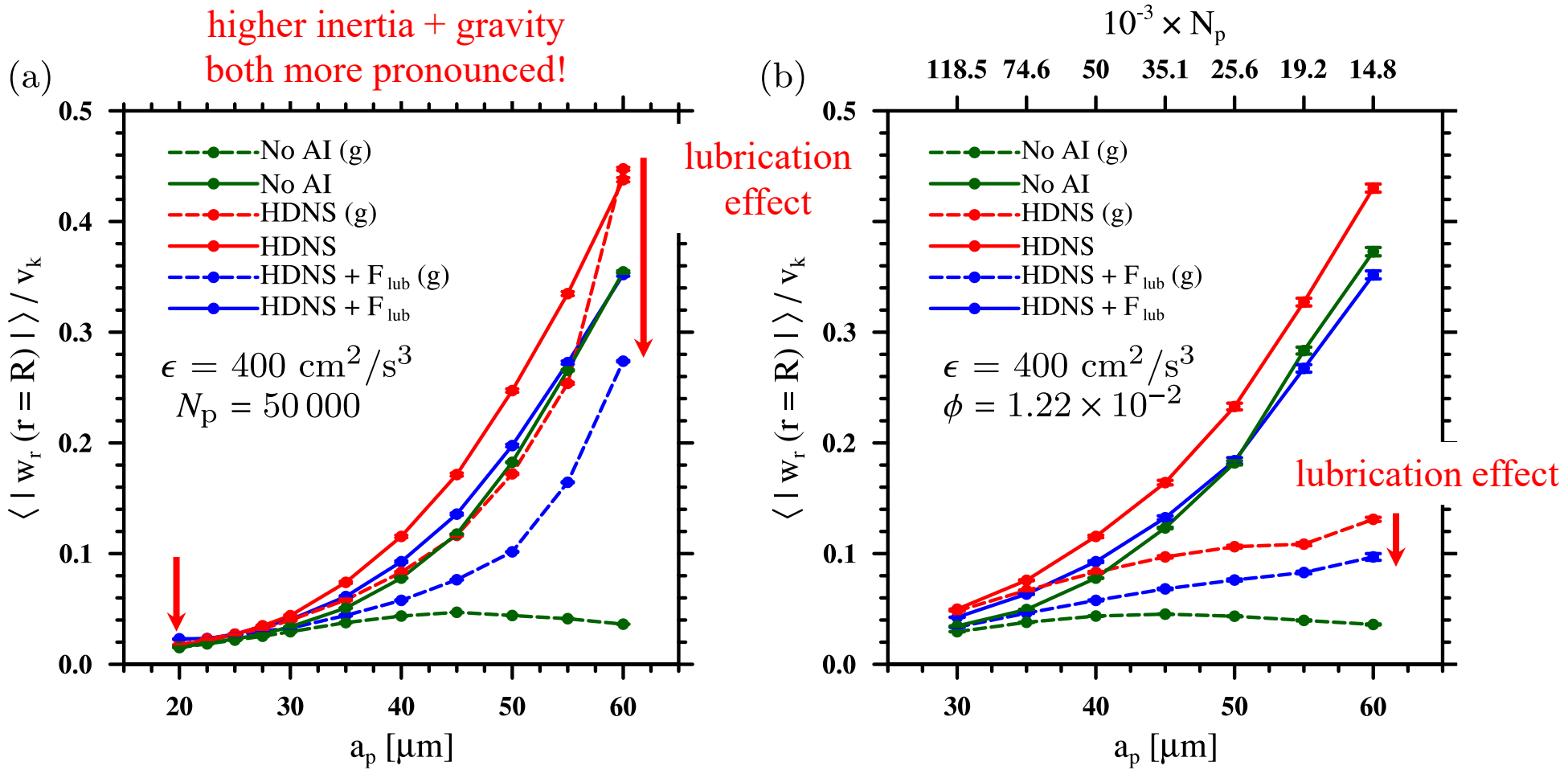

Comparison of at-contact RRV in case when there is aerodynamic interaction, both including and excluding lubrication forces, and when there is no aerodynamic interaction, all with and without gravity, for (a) the same number of droplets, $N_p = 50\,000$ and (b) the same mass loading, $\varphi = 1.22 \times 10^{-2}$ at the dissipation rate $\varepsilon = 400\ cm^2/s^3$.

Results

Comparison of the new *lubrication-included HDNS* with *standard HDNS* and simulations *without AIs*

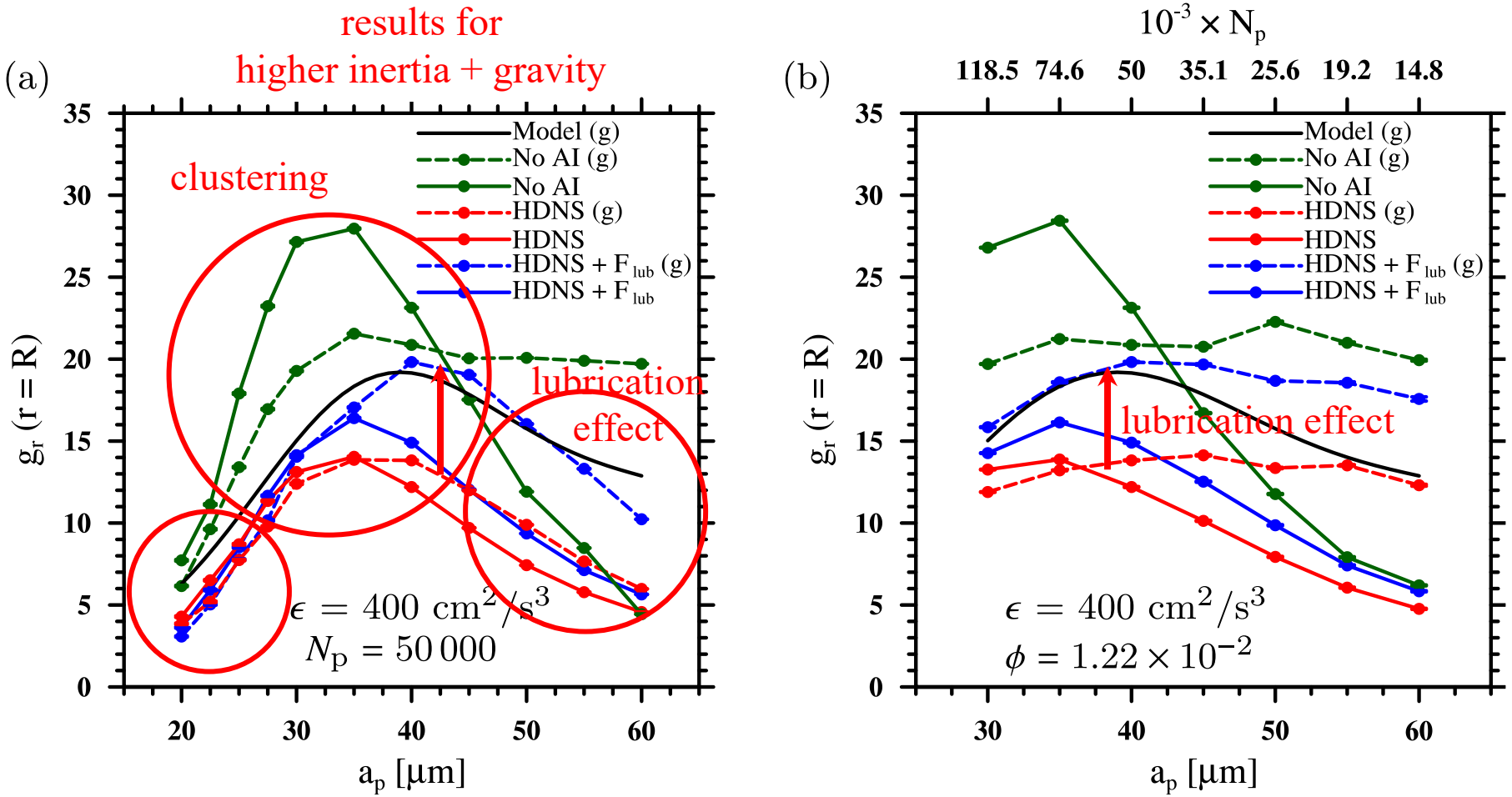

Comparison of at-contact RDF in case when there is aerodynamic interaction, both including and excluding lubrication forces, and when there is no aerodynamic interaction, all with and without gravity, for (a) the same number of droplets, $N_p = 50\,000$ and (b) the same mass loading, $\varphi = 1.22\times10^{-2}$ at the dissipation rate $\varepsilon = 400$ cm^2/s^3.

The empirical model of Ayala, Rosa & Wang (2008, (84) and (85) for $R_\lambda = 76.86$) is also included for comparison.

Results

Comparison of the new *lubrication-included HDNS* with *standard HDNS* and simulations *without AIs*

HDNS + F_{lub} vs HDNS (slight decrease)

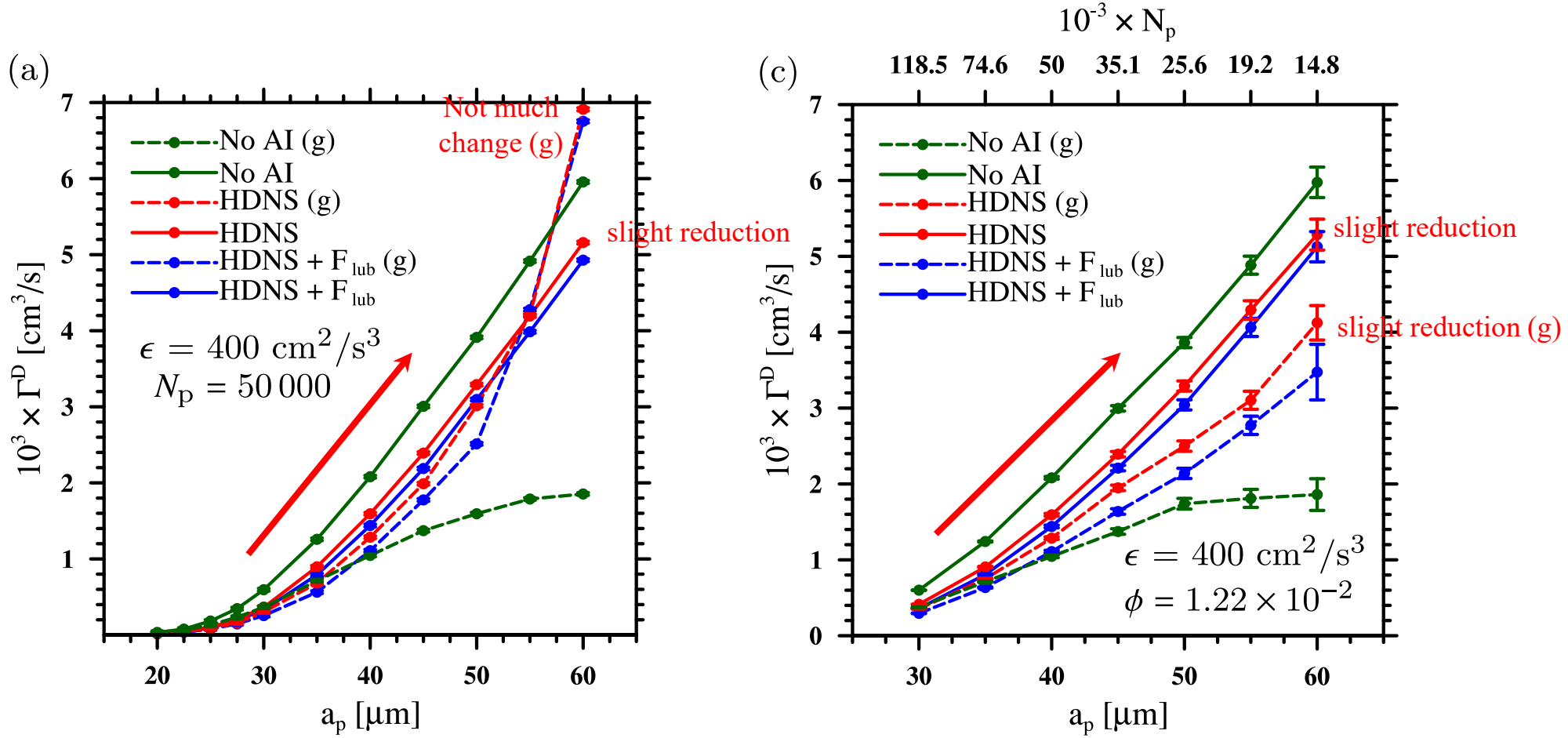

Comparison of the dynamic collision kernel when there is aerodynamic interaction, both including and excluding lubrication forces, and when there is no aerodynamic interaction, all with and without gravity, for (a) the same number of droplets, N_p = 50 000 and for (c) the same mass loading, $\varphi = 1.22\times10^{-2}$ at the dissipation rate ε = 400 cm^2/s^3.

Results

Corrections to kinematic formulations due to *non-overlapping droplets* condition

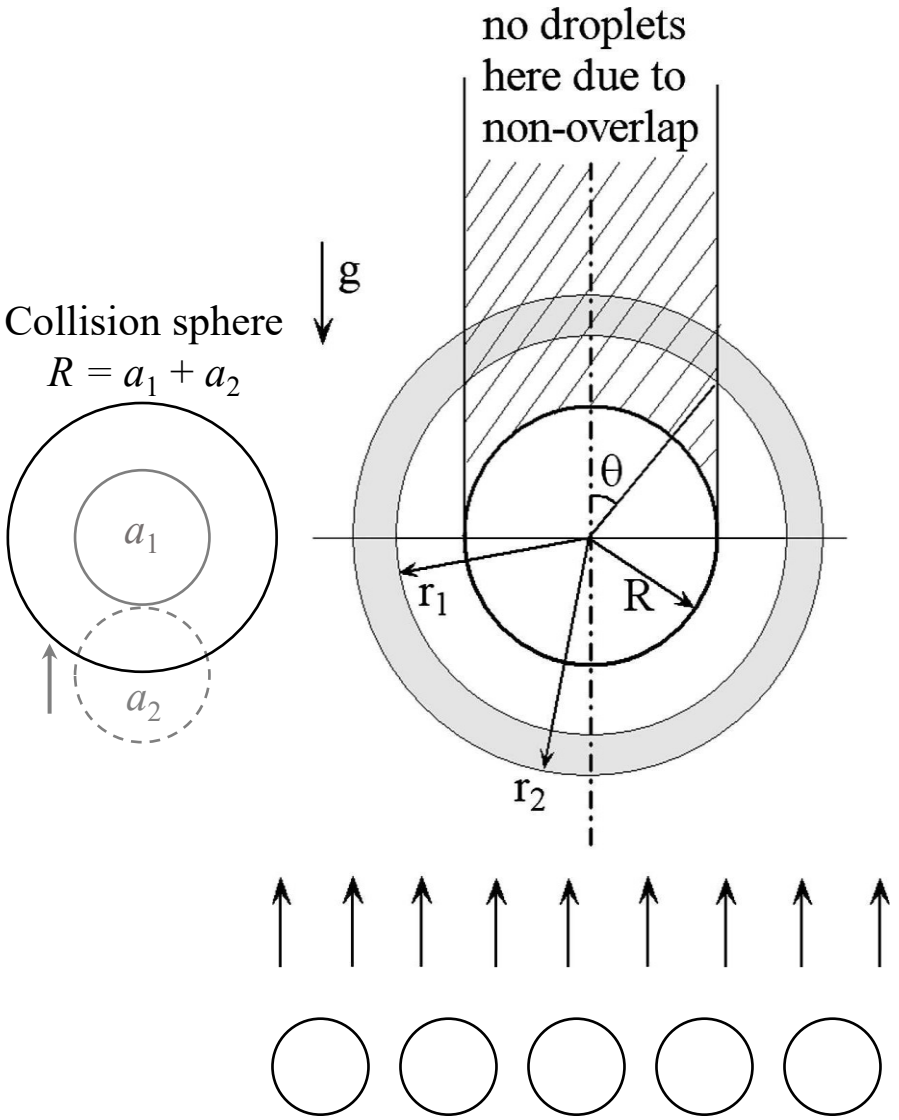

$$g_{12}(r) = \frac{4\pi r^2 - \int_0^{\theta} (2\pi r \sin\theta')(r\, d\theta')}{4\pi r^2}$$

$$= 0.5\left[1 + \sqrt{1 - (R/r)^2}\right],$$

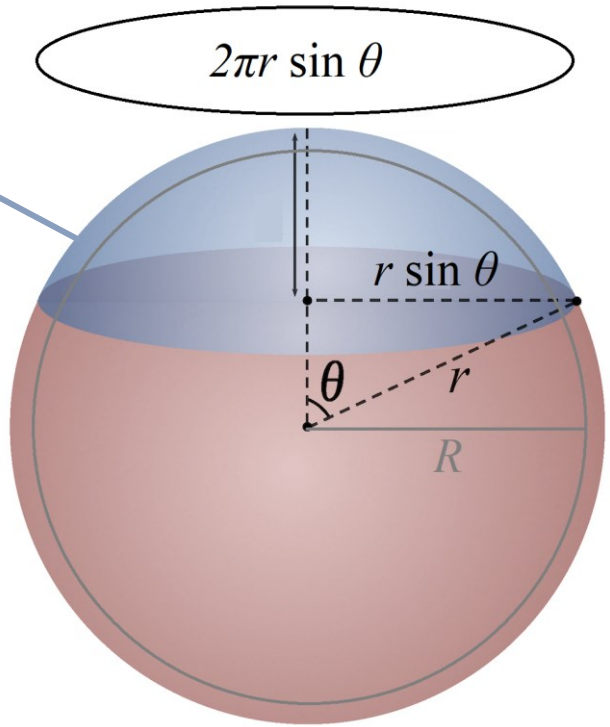

$$\langle |w_r(r)| \rangle = \left[\int_0^{\pi/2} (\Delta W \cos\theta')(2\pi r^2 \sin\theta'\, d\theta') + \int_{\theta}^{\pi/2} (\Delta W \cos\theta')(2\pi r^2 \sin\theta'\, d\theta') \right] \Big/ 4\pi r^2 g_{12}($$

$$= \frac{\Delta W}{2} \frac{2 - R^2/r^2}{1 + \sqrt{1 - (R/r)^2}}.$$

$$g_{12}(r_1, r_2) = \frac{\int_{r_1}^{r_2} 4\pi r^2 g_{12}(r)\, dr}{\int_{r_1}^{r_2} 4\pi r^2\, dr}$$

$$= 0.5 + 0.5[(r_2^2 - R^2)^{3/2} - (r_1^2 - R^2)^{3/2}]/(r_2^3 - r_1^3), \equiv C_g$$

$$\langle |w_r(r_1, r_2)| \rangle = \frac{\int_{r_1}^{r_2} \langle |w_r(r)| \rangle 4\pi r^2 g_{12}(r)\, dr}{\int_{r_1}^{r_2} 4\pi r^2 g_{12}\, dr}$$

$$= \frac{\Delta W}{2} \times \frac{1 - 1.5R^2(r_2 - r_1)/(r_2^3 - r_1^3)}{g_{12}(r_1, r_2)}. \equiv C_w$$

Results

Corrections to kinematic formulations due to *non-overlapping droplets* condition

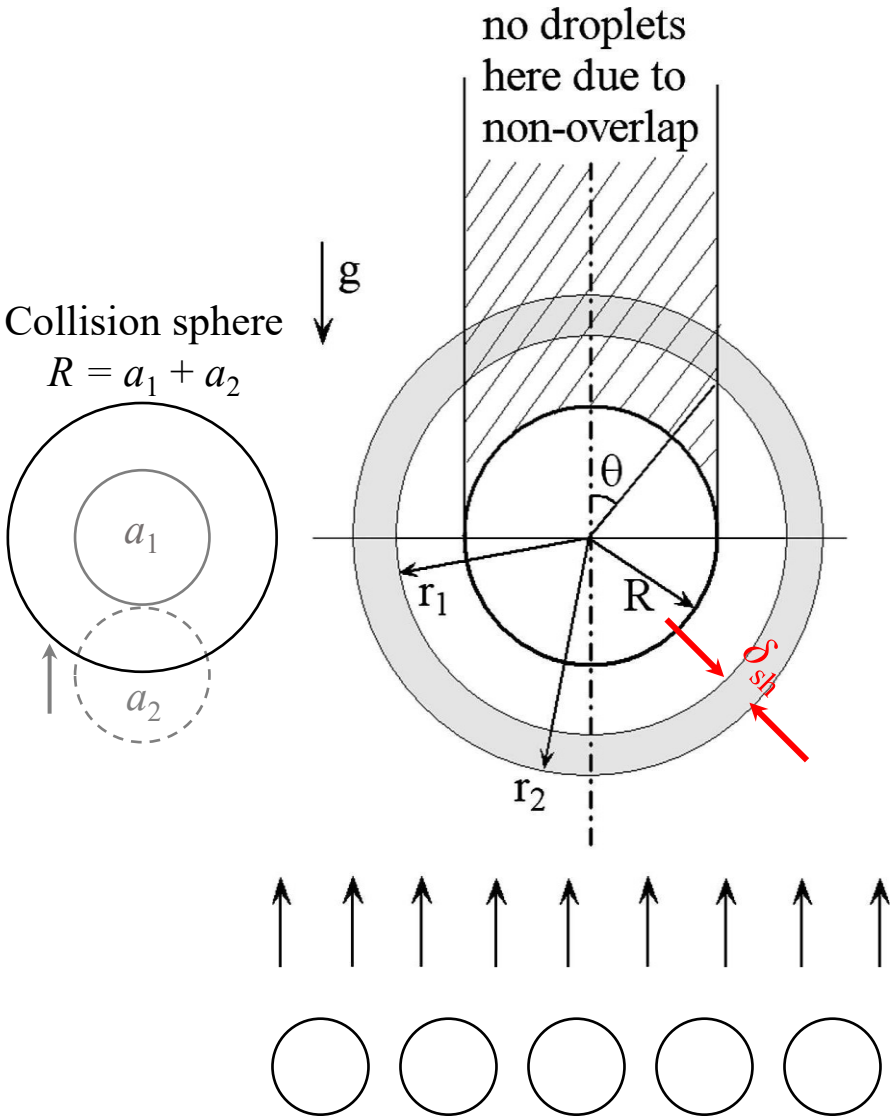

$$C_g\left(\frac{r_1}{R},\frac{r_2}{R}\right) = \frac{1}{2} + \frac{1}{2}\frac{\left(\left(\frac{r_2}{R}\right)^2 - 1\right)^{3/2} - \left(\left(\frac{r_1}{R}\right)^2 - 1\right)^{3/2}}{(r_2/R)^3 - (r_1/R)^3},$$

$$C_w\left(\frac{r_1}{R},\frac{r_2}{R}\right) = \left(1 - \frac{3}{2}\frac{r_2/R - r_1/R}{(r_2/R)^3 - (r_1/R)^3}\right) \Big/ C_g\left(\frac{r_1}{R},\frac{r_2}{R}\right),$$

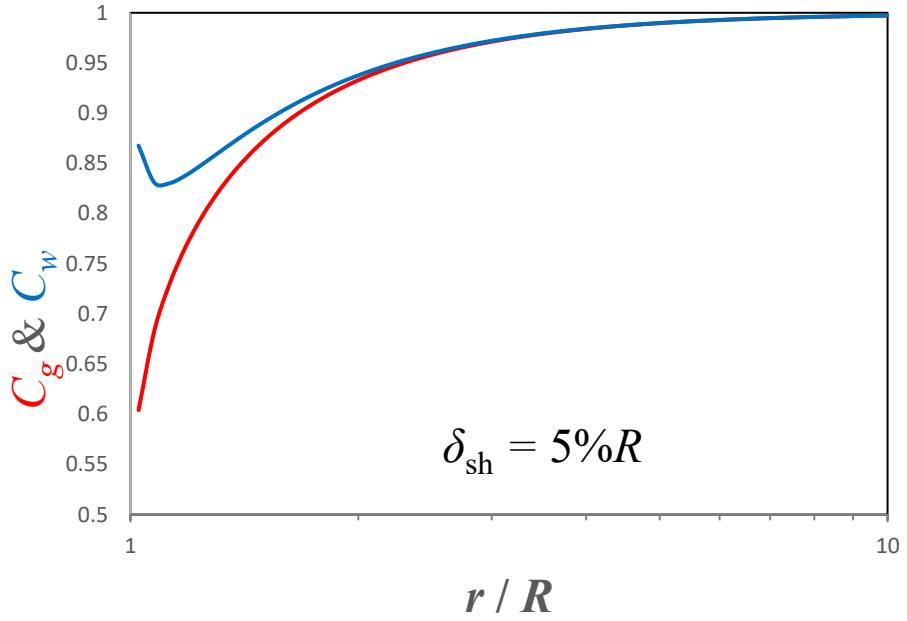

$$g_r^c(r/R) = g_r/C_g,$$
$$\langle|w_r^c(r/R)|\rangle = \langle|w_r|\rangle/C_w,$$

$$\Gamma^K = 2\pi R^2 \langle|w_r^c(r=R)|\rangle\, g_r^c(r=R)$$

Results

Validation of corrected kinematic formulations

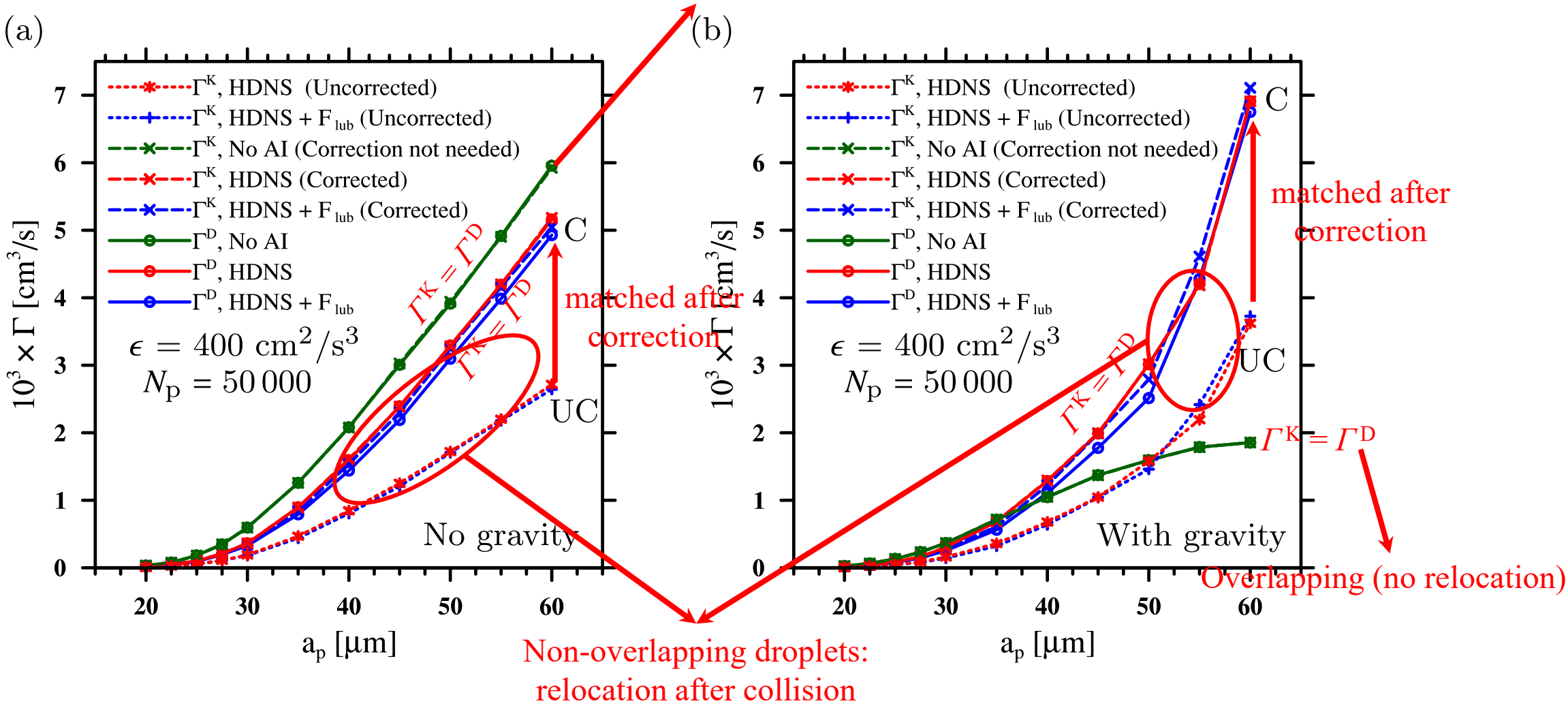

Comparisons between the collision kernel obtained from the dynamic formulation with that computed using the kinematic formulation, both before (UC) and after (C) applying corrections, when (a) gravity is not considered and (b) when there is gravity.

Results

Effect of particles number density and mass loading

Kinematics and dynamics are more sensitive to φ
with gravity and inertia (decorrelation)

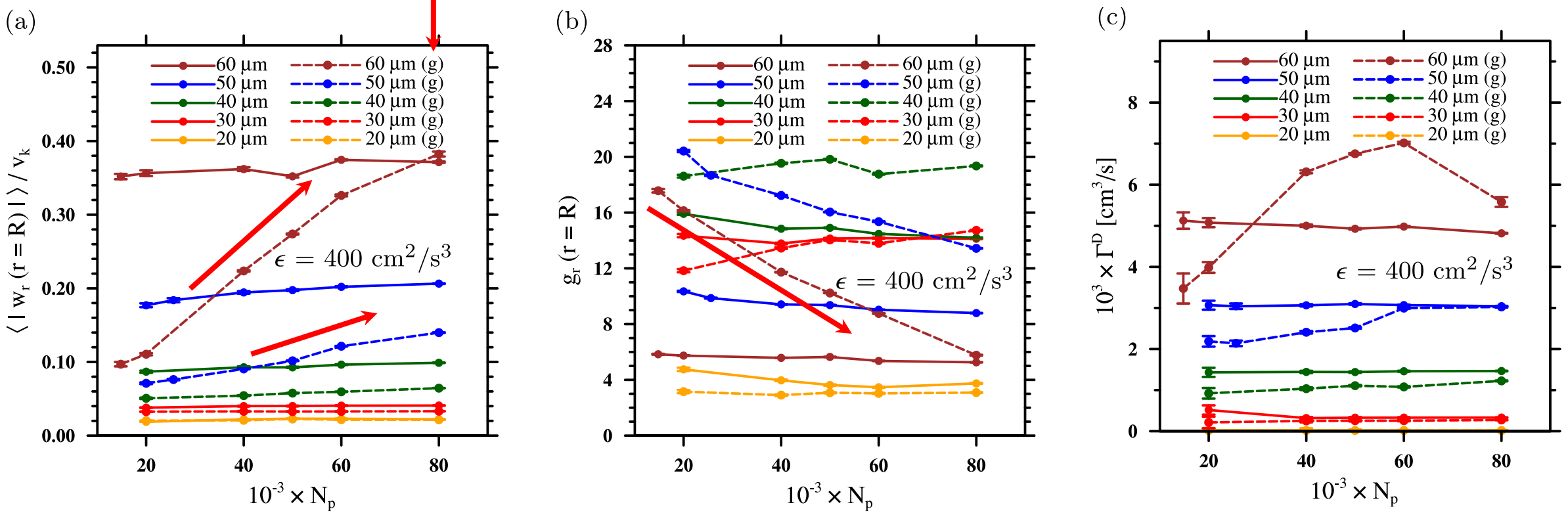

Changes in the at-contact (a) RRV, (b) at-contact RDF and (c) the dynamic collision kernel for the sets of droplets with different radii and numbers, i.e. different mass loadings.

Conclusions

- Due to the **non-linearity of lubrication forces**, at-contact kinematics strongly depend on the chosen **time step size**, while for larger separation distances there is not much change in kinematics by various choices.

- For **moderate-to-large inertia** droplets, considering **lubrication decreases RRV and increases RDF**, whereas for **small inertia** droplets the **RRV increases** which does not affect collision statistics due to very low clustering.

- By additionally considering **lubrication** effects, there is a **slight decrease** in the rates of **collision**.

- The effect of **lubrication** forces is **more pronounced** in systems with **larger energy dissipation** rates, especially if **gravitational** settling is considered.

- The **corrections** (due to relocation) applied to **kinematics** of droplet statistics can accurately **recover** values corresponding to **dynamic** formulation.

- When the **mass loading grows**, the kinematic collision statistics reveal an opposite trend, namely the **RRV increases** with the droplet number density, while the **RDF** monotonically **decreases**.

Thank you